9-29-2008

Induction of Apoptosis by Rubella Virus Non-Structural Replicase and Rescue by Capsid

Alison Elizabeth Kanak

doi: https://doi.org/10.57709/1059213

INDUCTION OF APOPTOSIS BY RUBELLA VIRUS NON-STRUCTURAL REPLICASE AND RESCUE BY CAPSID

by

ALISON KANAK

Under the Direction of Dr Teryl Frey

ABSTRACT

As a model for studying apoptosis associated with pathogenesis of congenital rubella syndrome, bicistronic rubella virus (RUBV) replicons expressing an antibiotic resistance gene in the presence (925-IN) or absence (IN-IN) of RUBV capsid protein (C) were constructed. Apoptosis was assessed by detection of caspase activation, chromatin fragmentation, and flow cytometry. 925-IN cells grew similarly to Vero, but -IN-IN cells demonstrated caspase activation, chromatin fragmentation and cell cycle arrest. Whereas Vero cells transfected with P150 exhibited rapid apoptosis not detected in transfected Vero cells stably expressing C, neither exhibited cell cycle alterations, indicating a cell cycle stall not associated with apoptosis. Finally, two human epithelial cells, HEK293 and A549, transfected with P150 failed to exhibit apoptosis, indicating that while replicon-transfected Vero cells are useful for studying apoptosis and cell cycle arrest, the results are not applicable to other cell types.

INDEX WORDS: Apoptosis, Rubella virus, Congenital Rubella Syndrome, replicon

INDUCTION OF APOPTOSIS BY RUBELLA VIRUS NON-STRUCTURAL REPLICASE AND RESCUE BY CAPSID

by

ALISON KANAK

A Thesis Submitted in Partial Fulfillment of the Requirements for the Degree of

Master of Science

in the College of Arts and Sciences

Georgia State University

2008

INDUCTION OF APOPTOSIS BY RUBELLA VIRUS NON-STRUCTURAL REPLICASE AND RESCUE BY CAPSID

by

ALISON KANAK

Committee Chair: Teryl Frey

Committee: Richard Dix
Zhi-Ren Liu

Electronic Version Approved:

Office of Graduate Studies
College of Arts and Sciences
Georgia State University
December 2008

ACKNOWLEDGEMENTS

I would first like to express my gratitude to my committee members, Drs. Liu, Dix, and Frey for their guidance, advice, encouragement, and support without which I never would have completed this degree. I would also like to thank to Dr Wen Pin-Tzeng for his patience and construction of cell lines and plasmids as well as express my deepest thanks to Heather Mousa and Suganthi Suppiah for their invaluable suggestions, help, insights, etc on how to function and succeed in a lab that I will never forget. Finally, a very special thank you to my husband Jason, my mom Susan, and my sister Heather whose continued support and encouragement have made it possible for me to achieve all of my dreams.

TABLE OF CONTENTS

LIST OF FIGURES

LIST OF ABBREVIATIONS

C – Capsid protein

CK – Citron kinase K

CPE – cytopathic effect

CRS – Congenital Rubella Syndrome

DI – defective interfering

DMEM – Dulbecco's minimal essential medium

EGF – epidermal growth factor

ER – endoplasmic reticulum

FBS – fetal bovine serum

GFP – green fluorescence protein

Ig – immunoglobulin

kDA – kiloDalton

MMR – Measles Mumps and Rubella

ORF – open reading frame

PBS – phosphate buffered saline

RDRP – RNA-dependent-RNA polymerase

RER – rough endoplasmic reticulum

RUBV – RUBV

TUNEL - Terminal Transferase dUTP Nick End Labeling

TdT – terminal deoxynucleotide transferase

CHAPTER I

INTRODUCTION

OVERVIEW

Since its first description in the mid-eighteenth century by Friederich Hoffmann, and subsequent descriptions by de Bergen and Orlow, [1] rubella has consistently been misunderstood. Initially believed to be a manifestation of scarlet fever or measles, it was not until almost one hundred years later that rubella was classified as a disease of its own [2]. It then required another hundred years for the causative agent of rubella, the rubella virus (RUBV), to be isolated in 1962 despite the fact that related members of the *Togaviridae* family, to which RUBV belongs, had been isolated years before [3]. Even though it has been almost 50 years since its isolation, knowledge of its molecular workings remains incomplete. Of course, since successful vaccination efforts have eliminated rubella from the majority of developed countries in the world [4], the question may be posed as to why this virus is even worth continued study. The answer to this question was addressed by ophthalmologist Norman Gregg in 1941 [10]. Dr. Gregg, after noticing a substantial number of congenital cataracts in babies born from mothers infected with rubella during pregnancy, described a wide variety of birth defects that we now know as Congenital Rubella Syndrome, or CRS. He went on to correlate the severity of the birth defects with how early in her pregnancy the mother was infected [5]. Given that CRS still exists today in most underdeveloped countries and that other infectious agents also cause birth defects, it is vital to understand the process by which infectious disease can interrupt development of fetal systems. Thus the goal of this research is to take steps towards understanding the molecular mechanisms of CRS with the hypothesis that it is the induction of apoptosis by RUBV that causes at least some of the birth defects associated with CRS.

RUBELLA, THE DISEASE

History

Rubella got its initial recognition in human history by being confused with measles and scarlet fever, due to the similarities in appearance of the rashes that these diseases produce. In fact, Friederich Hoffmann reported the first clinical description of rubella in 1740 without classifying it as a separate disease entity [6]. This description was later confirmed by Drs de Bergen and Orlow in 1752 and 1758, respectively [1]. It wasn't until 1814 that George de Maton proposed for the first time that rubella be classified as a disease distinct from both measles and scarlet fever [7]. The fact that all of these men were of German descent is why rubella came to be known as "German Measles". Rubella was given its official name by an English Artillery Surgeon in India, Henry Veale, in 1866. He decided on this name because in Latin rubella means "little red", thus correlating to the red rash that rubella produces [6]. Finally, 1881 saw the official recognition of rubella as a distinct disease at the International Congress of Medicine in London [2]. This official classification led to the beginnings of research on rubella. The early 1900's saw the beginnings of the idea that rubella was caused by a virus based on Alfred Hess' work with monkeys [8]. Hiro and Tosaka confirmed this hypothesis in 1938 by passing the disease to healthy children with filtered nasal washings of acutely infected individuals [5].

The cornerstone for rubella as a disease of significance, rather than a benign illness, was the discovery of its role in causing congenital birth defects. After a widespread epidemic of rubella in Australia in 1940, Norman Gregg noticed a strong correlation between children born with congenital cataracts and children born to women infected with rubella early in their pregnancy [9]. These observations led Gregg to publish his paper, *Congenital Cataracts Following German Measles in the Mother* in 1941, in which he described a number of congenital

defects that are today grouped together and classified as Congenital Rubella Syndrome (or CRS). In this paper, he also noted the positive correlation between the severity of the syndrome and the trimester during which the mother was infected, a correlation that has been confirmed [10]. The true impact of CRS was brought home in the rubella epidemic of 1964-1965, when 20,000 CRS cases occurred in the US and 1% of births in New York alone were diagnosed with CRS.

Finally, in 1962 the RUBV was isolated and identified simultaneously by two independent groups [11, 12]. Later in the same decade, live attenuated vaccines against this virus were generated and implemented in vaccination programs, first on its own and then ten years later as part of the triple vaccine against measles, mumps and rubella (MMR). Since the licensing of the rubella vaccine, the occurrence of rubella has gone from 12.5 million cases annually to nearly complete elimination in North America [5].

The Disease

Infection with RUBV results in a typically mild disease called rubella, German Measles, or three-day measles [13]. Due to vaccination efforts in the U.S., the incidence of rubella has declined precipitously and has changed from a predominantly childhood disease to one that mostly affects unimmunized young adults, usually of foreign origin [4].

Symptoms of rubella begin with a mild fever and swollen lymph nodes around the throat. Following this stage is the appearance of a rash resulting from the inflammatory response of the immune system with small pink or red spots on the face and chest that gradually spreads outward. At the time of appearance of the rash, antibodies against the virus become detectable and the infection is resolved. Many people infected with rubella have either very mild symptoms or none at all, but infection can also result in arthritis in adult women and congenital birth defects

in the fetus if the woman infected is pregnant [3]. Rarer sequelae include encephalitis and thrombocytopenia purpura.

The pathogenesis of RUBV infection is poorly understood because of the benign nature of the disease, because humans are the only known host and there is no animal model. The following are general steps in the infection cycle: RUBV replicates in the nasopharynx, both initially and following systemic infection, and is thus spread from person-to-person through direct droplet contact with the respiratory secretions of infected individuals. Upon entry into the respiratory tract, the virus infects cells of the respiratory epithelium and spreads to local lymph nodes, resulting in a primary non-cellular associated viremia that culminates in dissemination of the virus through the blood stream. Following this viremia, the virus is seeded in its target organs, such as the spleen and distant lymph nodes, where it undergoes a second round of replication [4]. At this point, approximately seven days after infection and about ten days before the onset of an immunopathologic rash, the virus can be recovered from the blood serum [9]. The maculopapular rash appears roughly three weeks after infection and appearance of the rash coincides with virus shedding from the nasopharynx. Shortly after the onset of the rash, viremia ceases and transformed lymphocytes as well as neutralizing antibodies can be detected in the blood. The virus continues to be shed from the respiratory tract, however, usually for less than a week, but occasionally for up to twenty eight days following the appearance of the rash [14].

Congenital Rubella Syndrome

While infection with RUBV only causes mild disease when contracted post-natally, it can cause severe birth defects (CRS) in a fetus, especially if infection is during the first trimester of pregnancy. Abnormalities induced can include deafness, blindness, mental retardation, and congenital heart defects [15]. In addition to these symptoms apparent at birth, individuals diagnosed with CRS and followed for 50 years also had a predisposition towards late-onset illnesses such as insulin-dependent diabetes, thyroid dysfunction, and panencephalitis [16].

It is believed that it is during the period of viremia in the mother that the virus infects and then crosses the placenta to infect the fetus. The exact mechanisms of how the virus crosses the placenta have not been elucidated. Since the fetus has not yet developed its immune system, it must rely on antibodies secreted by the mother who is in the process of producing antibodies of her own against the virus. Thus, the titer of maternal antibodies is too low and transfer of these antibodies is too inefficient due to the predominant production of antibodies being IgM, which cannot cross the placenta, to be able to effectively combat the virus that is now in the fetus' system. Since the fetus has no adaptive defense system against the virus at this time in development, RUBV can infect and damage any organ system as well as maintain a chronic nonlytic infection in the fetal cells. In fact, following infection early in pregnancy, the virus persists and can be recovered for up to a year after birth [3]. This persistence is in spite of the eventual induction of neutralizing antibodies in the fetus as well as the fact that immunological tolerance never develops [17]. It is believed that this persistence could be promoted in part by the presence of DI particles as well as the lack of development of certain aspects of the cell-mediated immune response. However, the exact component of cell-mediated immunity has not been identified [16].

The pathogenesis of CRS varies widely, from no apparent defects to multiple systems damage, and the central mechanisms are only poorly understood. Two common features however, are reduced size of affected tissues, presumably due to reduced cell numbers, and angiopathy of early placental and embryonic tissues that interferes with fetal blood supply. The affects of these two pathways are manifested in various ways in the fetus. One of the most affected organs is the eye. Here, cellular death by necrosis and apoptosis both seem to play roles in either the prevention of lens development or the damage of tissue already established which leads to the generation of cataracts [3, 16]. When Norman Gregg was making his observations of fetal cataracts tied to rubella in 1941, he also noticed that these cataracts affected all but the very outermost layers of the lens of the eye. This would suggest that the formation of these cataracts began very early in the development of the eye [10]. These assumptions were confirmed through experimentation with and observation of necrosis in lens fibres obtained from neonates dying 3 weeks to 6 months after birth due to CRS related complications [16].

While the pathogenesis of CRS is not understood, it is very clear that the time of infection with regards to the stage of pregnancy is extremely important with regards to CRS developing in the fetus. In an experiment to determine the correlation between stage of pregnancy and severity of CRS, pregnant women who had been exposed to RUBV allowed their babies to be tested for RUBV infection, either through the detection of RUBV-specific IgM immediately after birth or the detection of persistent IgG after the first year of life, two common means of diagnosing CRS. Of these, 81% of the infants exposed during the first trimester tested positive for these antibodies. For mothers exposed during the second trimester, infection in infants dropped to 67% and in the third trimester infection was only seen in 35% [18]. The reasons for this correlation between pregnancy stage and the ability of the virus to cross the

placenta are still unknown. However, it is possible that developmental changes in the placenta itself could lend to the increased defense against fetal RUBV infection in later stages of gestation.

Toward understanding the pathogenesis of CRS, two areas of experimentation have been pursued, namely the interference of RUBV with growth and division of infected cells [19, 20] and the improper induction of apoptosis in infected cells [21]. A number of studies have investigated the cellular effects of a persistent RUBV infection in tissue culture, a persistence that can be correlated to persistent fetal infection by RUBV. RUBV persistence is maintained without a proviral DNA intermediate, as is seen in viral latency infections, even in the presence of neutralizing antibodies in the culture medium, which also correlates with persistence in the infected fetus from late in gestation when the fetus develops the ability to make antibodies through birth [19, 20, 69-74]. The mechanism by which RUBV maintains these persistent infections remains unclear, with hypotheses including possible roles of interferons and a more promising suspicion of the role of DI particles, virus mutants which interfere with virus replication and attenuate pathogenicity, in the establishment and maintenance of these persistent infections [19, 20]. However, it is evident that these infections do exert negative consequences against the growth of the cell culture. Most apparent are the results reported by Yoneda's group in 1986 in Japan [22]. It was established that human embryonic mesenchymal cells derived from the palate (HEMP cells) exhibit a high sensitivity to epidermal growth factor (EGF) that results in high levels of collagen production and cell growth. However, once these cells are infected with RUBV and a persistent infection is established (HEMP-RV), the cells lose their sensitivity to EGF. Regardless of the levels of EGF applied, HEMP-RV cells remain unresponsive to EGF. It was also noted that this insensitivity was due to physiological changes in the cells which

inhibited differentiation resulting in their inability to internalize EGF once it was bound to surface receptors or to respond to EGF-triggered signaling stimuli [22]. Thus, cells persistently infected with RUBV were found to have growth inhibition most likely as a result of deregulation in cell signaling pathways. Given that this cell line is a diploid derivative of an embryonic line, it can be inferred that these differentiation and growth inhibition phenomena triggered by persistent RUBV infection could correlate to the decrease in tissue size and development seen in fetuses infected with RUBV. Correlating to these findings, it was also shown that post-infection with RUBV certain fibroblast cell lines may actually secrete growth inhibitors into the population [23].

While Vero cells infected with RUBV can produce high titers of virus and can exhibit cytopathic effect (the basis of plaque formation), they have also been shown to be able to establish persistent RUBV infection [19]. Following infection, there a 20-30% decrease in cell survival between 24 and 48 hrs post infection can be observed, the time period where the RUBV-induced cytopathic effect was first observed [14]. Cytopathic effect was shown to be due to the induction of apoptosis in Vero cells. It was determined that apoptosis was the cause of cell death after it was found that these cells exhibited such apoptotic hallmarks as chromatin fragmentation and production of a DNA ladder upon gel electrophoresis, the binding of Annexin-V following disruption of the cell membrane, and inhibition of progression through the cell cycle [21]. Nevertheless, some cells have been observed to survive and to grow into a persistently infected culture. However, even during persistent infection, cytopathic effects can be observed. Under optimal growth conditions following subculturing, the monolayer of persistently infected cells remained subconfluent, while 40%-50% of cells detached and died [21]. Eventually, with passage of the culture, CPE was less profound which may be due to selection of attenuated virus

mutants and DI RNAs. Significantly, persistently infected Vero cells cannot be cured by inclusion of neutralizing anti-rubella antiserum in the medium, which correlates with the inability of antibodies to eliminate persistence in an infected fetus before birth [20]. An interesting correlation to this could be achieved if similar results were obtained after adding C1 component of complement or lymphocytes were added to the media as these are also primary host defenses to RUBV infection.

RUBV-induced apoptosis has been studied in a number of cell cultures, most extensively in Vero, BHK21 and RK13 cells with a generalized conclusion that while RUBV definitely induces apoptosis [21, 80] it does so through different mechanisms and to different levels in different cell lines. For example, in 1999, Megyeri observed that p53, a pro-apoptotic tumor suppressor host protein associated with repairing extensive DNA damage, expression is elevated in Vero cells during infection with RUBV and that dominant-negative p53 mutants transfected into Vero cells during infection decreased the level of apoptosis and thus concluded that RUBV induces apoptosis through a p53-dependent mechanism [81]. However, in the same year Hofmann determined that rubella induces apoptosis through p53-independent pathways in Vero cells and this conclusion has been supported by Domegan's 2002 study in rat neuronal cells [80,79]. The apoptosis pathways activated by RUBV are not the only aspects in dispute. While levels of cytotoxicity in Vero cell have been mapped to the RUBV non-structural proteins [35] and this thesis confirms this finding in Vero cells, C was found to induce apoptosis in RK13 cells as long as it contains the C-terminal 23 amino acid sequence which anchors it in the membrane [78]. Finally, Duncan et al [77] showed that while RUBV induces apoptosis in Vero, BHK-21, and RK13 cells it does so to varying levels with RK13 cells showing the most robust apoptotic response and BHK-21 showing the lowest levels of apoptosis induction.

RUBELLA, THE VIRUS

RUBV is the sole member of the *Rubivirus* genus within the *Togaviridae* family. Other well-known viruses in this family include mosquito-borne Semliki Forrest Virus and Sindbis Virus which belong to the *Alphavirus* genus. RUBV is an enveloped, single-stranded, positive-sense RNA virus with a spherical morphology ranging in diameter from 70-80 nm (Fig. 1). Beneath the lipoprotein envelope is an electron-dense spherical core ranging from 30-35 nm in diameter. Within this core resides the RUBV genome. The core, or capsid, is formed by multiple copies of the viral capsid protein [24] which is nonglycosylated and associates with the viral RNA. Projecting from the envelope are spikes, composed of the virus glycoproteins, E1 and E2 that exhibit hemagglutination activity and are the moieties which make initial contact with the cell to be infected and against which neutralizing antibodies interact. While RUBV is categorized within the *Togaviridae* family, it is serologically distinct from the rest of the members of this family, justifying its classification as the only member of the *Rubivirus* genus. The multiplication of this virus family is highlighted by reliance on a subgenomic RNA for the translation of the structural proteins (Fig. 2). Initially after infection, the virion RNA, which is capped and polyadenylated, serves directly as the mRNA for translation of two nonstructural proteins, P150 and P90, the genes for which lie in the 5' two-thirds of the genome. The nonstructural proteins, which are replicase proteins, then copy the virion RNA into a negative-strand RNA. It is from this negative-strand RNA that both positive-strand RNAs, the genomic and subgenomic RNA, are templated. The subgenomic RNA, consisting of sequences from the 3' end of the genomic RNA, is translated to produce the virion structural proteins, C, E2, and E1 [13].

RUBV STRUCTURAL PROTEINS

As can be seen in Figure 2, RUBV codes for its structural proteins using the 3' ORF. This ORF is accessed using a subgenomic RNA which is initiated on the negative-sense copy of the genome using an internal promoter. This ORF is translated into a C-E2-E1 polyprotein that is co-translationally cleaved into its components. The RUBV capsid protein (C) has been shown to be a dynamic, multi-functional protein. On SDS-Page, C migrates as a doublet with its lower band consistently being the more intense of the two bands. It is believed that this phenomenon is due to the differential phosphorylation events that occur on the capsid [13]. Its migration indicates its molecular weight to be approximately 33kDa and the protein contains 300 amino acids. In the nucleocapsid, C exists as a nonglycosylated, phosphorylated homodimer linked by disulfide bridges. Its amino terminal half, which contains a large number of arginine residues, is extremely hydrophilic. Due to the overall positive charge lent by the arginines in this domain, it is believed that this half of the protein is responsible for binding the genomic RNA. A specific 29-nucleotide sequence in the genome RNA [25] has been identified as a packaging signal which initiates capsid formation. The carboxy-terminal 23 residues of C are highly hydrophobic, and they are the signal sequence for translation of the E2 glycoprotein as a membrane protein into the lumen of the ER. This stretch remains attached to C following cleavage by cell signalase and appears to be responsible for anchoring of C in cell membranes during replication. In addition to forming the capsid within the virion, C's activities include binding to the genomic RNA and regulating the processes of RNA replication and virion assembly, apparently through differential phosphorylation [25], modulation of genomic and subgenomic RNA synthesis [26], as well as interactions with mitochondrial proteins such as p32 that may cause the perinuclear clustering of mitochondria observed in infected cells [27, 28]. The capsid protein has also been shown to

interact with the P150 nonstructural replicase protein, although how this binding plays a role in any of these functions has not been elucidated [29]. Finally, the C protein has been shown to induce apoptosis in RK13 cells [78].

Not much more is known about RUBV' other structural proteins, E1 and E2, than is known about C. As can be seen in Figure 2, E2 and E1 are located downstream of capsid in the structural ORF with E1 being at the very end of the coding sequence. The E1 gene codes for 481 amino acids while the E2 genes codes for 282 amino acids. During SDS polyacrylamide electrophoresis, E1 migrates as a distinct band at 59kDa while E2 migrates as a smear from 44-50kDa. Since all regions of this smear yielded identical amino acid sequences, it is believed that this smear results from differential glycosylation of the E2 protein that result in different apparent molecular weights [13]. Both of these proteins contain disulfide bonds integral to their structure as well as N-glycosylation sites. Interestingly, changes in the N-glycosylation sites have been found in attenuated viruses versus their wild type counterparts, and it could be possible that glycosylation plays a pivotal role in vaccine attenuation [13]. In addition to N-glycosylation, E2 also contains O-linked glycosylation. Finally, both proteins have single predicted transmembrane sequences near their carboxy termini [13].

Thus far, only theories can be proposed for the definite mechanisms of action of these two proteins. It is well known that they form the spikes on the outside of the virion's envelope, and it appears that E1 forms a homodimer with itself as well as a heterodimer with E2 in the spikes given that it is possible to immunoprecipitate both of these moieties with E1-specific antibodies. It appears that E1 is primarily exposed on the virion surface until it is subjected to low pH, at which point E2 becomes the primarily exposed protein. The functions of E1 include

hemagglutinin (indicative of binding to cell receptors) and membrane fusion following exposure to low pH. Most neutralizing epitopes also reside on E1 [13].

RUBV NONSTRUCTURAL PROTEINS

The RUBV non-structural proteins carry out the functions required for replication of the viral genome, and they are encoded and translated from the 5' proximal open reading frame. This ORF codes for a P200 polyprotein that is later cleaved into the two nonstructural replicase proteins, P150 and P90 [13]. Not much information has been gathered with regards to the structures of these proteins, and it has proven challenging to isolate their functions since RUBV does not produce a large amount of these proteins and does not shut down host protein synthesis; in fact, host proteins are frequently found aiding the replication of the virus. This was first demonstrated by the inhibition of viral replication following the addiction of actinomycin-D (an inhibitor of DNA-dependent RNA polymerase activity) [83]. In addition, the termini of the RUBV genome are capable of forming stable stem-loop structures that have been demonstrated to bind go host cellular proteins such as calreticulin [84, 85].

Helicase and RNA-dependent-RNA polymerase (RDRP) activities reside within the P90 replicase protein. Within the RDRP domain, a GDD motif was located that is critical to its function. Mutating any of these amino acids, to an alanine for example, results in the loss of replication of the genomic RNA [30]. In addition to its replication activities, P90 has been found to interact with host Citron-K kinase (CK). CK has been associated with interruptions in the cell cycle resulting in cells stalling just after S phase and it has been proposed that this stall results in tetraploidy, leading to subsequent degradation of cells and tissue, which could be a cause of

RUBV' teratogenic affects [31]. However, P90 lacks the putative binding domain for CK, and thus their colocalization might not be indicative of interaction.

The P150 protein contains a methyltransferase/guanylyltransferase domain used for capping the genomic and subgenomic RNA as well as a cysteine protease domain with a catalytic site consisting of Cys-1151 and His-1272 which performs cleavage of the P200 precursor at Gly-1300-Gly1301 [32]. This protease activity is contingent on the protein attaining its proper three-dimensional shape, and this shape is considered dependent upon the binding of cations to the protein [33]. The function of P150 is highly susceptible to mutations anywhere in the N-terminus with the exception of nucleotides 1685-2192 [34]. This region, labeled NotI and composing 5% of the genome, seems to be dispensable, as was shown by its ability to still replicate the genome in the presence of a helper virus [34]. This finding was later found to be due to the interaction between P150 and C as C has the ability to "rescue" this deletion that is lethal in its absence [26]. After synthesis, P150 first associates with small vacuolar structures approximately 24 hours post infection and then later, at 48 hpi, moves to associate, along with the capsid protein, in long filamentous structures that co-localize with the cellular tubulin network [29]. Interestingly, determinants of cytopathogenicity in cell culture and arithritogenicity in synovial explants were mapped to the P150 gene [35].

RUBELLA-VIRUS REPLICATION CYCLE

Despite the fact that the sole host for RUBV is humans, a number of permissive cell lines from several species, both primary and continuous, have been used for scientific study. However, in most of these cell lines, RUBV only produces low titers and induces little to no cytopathic effect (CPE). RUBV grows well in two particular epithelial cell lines: BHK-21 (hamster kidney)

and Vero (African green monkey kidney). These cell lines probably produce such high titers of the virus because both lack a functional interferon system [36], and thus the cells lack an intrinsic defense system against viruses. The lack of an interferon system alone, however, is not completely what allows these cell lines to accommodate RUBV as the virus is also able to establish persistent infections in cell lines with active interferon systems [36]. RUBV infection has also been studied in RK13 (interferon competent rabbit kidney cells) in which a dramatic CPE is induced, but virus titers produced are lower than in BHK or Vero cells. Even in the most permissive cell lines RUBV replication is extremely slow when compared to other RNA viruses, with a 12 hour eclipse period and production of peak titers at 36 to 48 hours post-infection [37]. The CPE observed as a result of RUBV infection usually appears between 36 and 48 hours post-infection as well and consists of an increased refractive index, cell rounding and detachment, and debris adhering to the monolayer [13].

In the 1970's multiple groups found that attachment of RUBV to host cells is fairly rapid compared to other RNA viruses with adhesion occurring anywhere from 30 minutes to 3 hours post-infection [13]. Despite the number of cell lines that RUBV can infect, its primary cellular receptor has not yet been elucidated. It is typical of most enveloped mammalian viruses to undergo receptor-mediated endocytosis after attachment (Fig. 3). Once endocytosis has occurred, the endosomal pH is rapidly lowered. This results in a conformational change in the viral glycoproteins to allow fusion of the virus and endosomal membranes and subsequent release of the viral genetic material into the cytoplasm. This pathway of steps has been demonstrated experimentally for RUBV infection [38]. Also, it has been shown that exposing RUBV to low pH does induce membrane fusion activity with a concomitant conformational change in its glycoproteins [39], supporting the theory that this is, in fact, the pathway by which the virus

enters the cell. The RUBV C protein also undergoes conformational changes under low pH that could expose its hydrophobic COOH region that then binds to the membrane of the endosome, possibly assisting in dissociation of the capsid following entry. Finally, Lee's group showed with thin-section transmission electron microscopy that RUBV appears to enter cells via endocytic mechanisms [40].

Once the RUBV genetic material has been released into the cytoplasm, replication of the genome begins. Because the genome is capped and polyadenylated, it is recognized by the cell as a messenger RNA, and thus translation starts immediately to produce the P200 polyprotein that is encoded by the 5' proximal ORF. Unlike many animal viruses, RUBV does not shut down host protein synthesis, either at this point in the replication cycle or later. Interestingly, the AUG that signals where translation starts is not the AUG that is closest to the 5' end, but rather is 37 nucleotides downstream from the first AUG in the genomic sequence at nt 3. In fact, translation from an AUG this close to the 5' end of a mRNA tends to be highly inefficient and translation of a functional protein from this AUG would be precluded by presence of downstream in-frame stop codons [13]. This AUG was also successfully removed without affecting virus replication to any detectable extent [41]. Once the polyprotein is made, its embedded protease self-cleaves it into the two non-structural proteins, P150 (at the amino terminus of the precursor) and P90 (at the carboxyl terminus).

After cleavage of the P200 precursor, P150 and P90 function as a complex to transcribe a full-length negative-sense RNA using the genome as its template (the catalytic RDRP resides in P90). Two positive-sense RNA species are produced from this negative-sense transcript: a copy of the entire genome that is later packaged into mature virus particles as well as a "subgenomic" piece containing sequences from the 3' end of the genomic RNA, including the 3' proximal ORF

encoding RUBV' structural proteins. The subgenomic RNA is capped and polyadenylated and can be directly translated to produce the structural proteins [13].

Once the subgenomic RNA has been produced, it is used to translate the 3' structural ORF into a P110 polyprotein precursor whose gene order is NH_2-C-E2-E1-COOH [42]. The glycoprotein components of this polyprotein are translocated to the lumen of the ER by two distinct signal sequences that are upstream from the amino termini of E2 and E1. As translation occurs, ER P110 is cleaved by a cellular protease in the lumen of the ER to produce C, E2, and E1, and thus the P110 species is never observed in infected cells [43]. A unique characteristic of RUBV is the retention of the E2 signal peptide on the carboxy terminus of C and the E1 signal on E2. In particular, the E2 signal retained by C allows association of C with membranes [44]. Following the cleavage of P110 into the individual structural proteins, E1 and E2 form a heterodimer linked by disulfide bridges and hydrophobic interactions at the same time that C forms homodimers linked by disulfide bridges [45]. Upon the completion of dimer formation E2-E1 move through the ER into the Golgi [13]. Unlike alphaviruses, which use only the plasma membrane as a site of maturation [46], rubella virion maturation takes place in the Golgi, rough ER, and cytoplasmic vacuoles [47, 48].

The exact process of virion assembly is thus far unknown. However, it is well established that virus RNA replication takes place in "replication complexes", vacuoles which seem to form under the surface of viral-modified endosomes and lysosomes. The converted organelles, known as "cytopathic vacuoles", recruit other cellular structures such as the RER, Golgi, and mitochondria to the site of replication, thus providing the replication complexes with all the energy, ribosomes, and protein processing required for successful, rapid replication [40, 49, 50, 51]. These complexes allow the viral RNA to be replicated within the membrane-bound vacuoles

with subgenomic RNA immediately translated by the RER and genomic RNA handed off to be packaged by C in association with the Golgi [3]. Once the viral RNA is packaged inside the capsid, the virion buds through the Golgi membrane containing E1 and E2 and into the lumen of the Golgi. Virions are eventually released from the cell via exocytic pathways.

APOPTOSIS- Programmed Cell Death

All mammalian cells have a finite lifespan, and the mechanisms employed to execute this are apoptosis and autophagy. While cells also die through means of necrosis, it is advantageous to employ apoptosis and autophagy as mechanisms of cell death for maintenance purposes due to the lack of immune and inflammatory responses induced by these mechanisms of cell death as opposed to the extensive inflammatory and immune responses induced by necrosis. Apoptosis, or programmed cell death, was first discovered by Carl Vogt in 1842 and was confirmed by Walther Flemming 40 years later. Highly controlled and regulated, apoptosis is signaled by such factors as developmental programs, cell damage, viral infection, environmental stress such as starvation, and as a preventative against cancer. Signals for initiating apoptosis can come either from within the cell itself or from external environmental stimuli. In the case of cell damage and viral infection, the signal for apoptosis is the cell's altruistic attempt to eliminate itself as a source of nutrient deprivation or viral production that could strain the organism itself without inducing inflammation pathways such as necrosis would. Primarily, however, apoptosis is the process through which cell numbers in an adult organism are kept relatively constant [52]. Apoptosis is highly regulated, and it is characterized by very specific morphological and biochemical changes within the cell. Common morphological features are cell shrinkage,

chromatin fragmentation, one of the first steps in apoptosis, inversion and blebbing of the plasma membrane, and the eventual fragmentation of the cell into what are known as apoptotic bodies. These apoptotic bodies are then consumed by neighboring cells [53]. The biochemical hallmarks of apoptosis are chromatin fragmentation, loss of mitochondrial membrane integrity, and overproduction of regulatory proteins involved in the stimulation and termination of apoptosis.

Regulation of apoptosis is pivotal to tissue health as well as development and thus must be highly specific. There are two main pathways which can signal the induction of apoptosis: intrinsic and extrinsic [54, 55]. The intrinsic pathway is initiated either by internal developmental signals or severe cell stress such as extreme DNA damage, a defective cell cycle, detachment from the extracellular matrix, hypoxia, or loss of cell survival factors. The beginning of this pathway is marked by the release of cytrochrome C as well as other pro-apoptotic proteins from the mitochondria [54, 56]. In contrast, the extrinsic pathway is initiated through the binding of a pro-apoptotic ligand, such as FAS ligand, to its pro-apoptotic receptor, such as FAS, which then undergoes a conformational change that recruits FADD and begins a signal cascade. The intrinsic and extrinsic pathways overlap in that both lead to the activation of cellular caspases [56, 57]. Caspases are the master regulators of apoptosis, and they are cysteine proteases that, once activated through the caspase signaling cascade, destroy cellular proteins that are critical to cell survival. There are two tiers of caspase activation during apoptosis: initiator caspases, consisting of caspases 2, 8, 9 and 10, are activated by pro-apoptotic ligand binding and cell stress and they in turn activate effector caspases, consisting of caspases 3, 6, and 7, which carry out apoptosis in a gradually expanding cascade [56, 57].

Apoptosis is a pivotal event during the development of mammals, frequently considered as pivotal as cell proliferation. It aids in regulation of cell numbers and remodeling tissues and

organs in the developing fetus [15]. This process of development through apoptosis has been compared to an artist creating a sculpture by the gradual removal of stone [58]. The development of tissues through the removal of cells is evidenced in the formation of ducts, tubes, digits, the fusion of palatal shelves, and the closure of the neuronal tube through the systematic removal of superfluous tissues [59-61]. Without this process, for example, humans would have webbed fingers and toes. It is also thought that without this process the establishment of the peripheral nervous system would never proceed [58]. However, despite these positive effects of apoptosis during fetal development, the excessive induction of apoptosis has been shown to cause abnormalities and birth defects [62]. It has been shown that excessive cell death consistently occurs in fetuses preceding the appearance of structural anomalies. In fact, studies have shown that known teratogenic environments such as hypo- or hyperthermia, ionizing radiation, and alkylating agents in the mother induce apoptosis in target fetal organs resulting in repercussions in correlating organs such as exencephaly, microcephalyy, and microphthalmia [62].

As discussed above, in the cell lines in which RUBV induces cytopathic effect, it is due to induction of apoptosis.

RUBELLA VIRUS REPLICONS

Given the relative instability of RNA species, it has become invaluable in the study of RNA viruses to use reverse transcriptase to construct DNA copies (cDNA) of viral RNA genomes. Such cDNAs can be incorporated into plasmids for amplification and mutagenesis. If the cDNA is placed in a plasmid with an RNA promoter upstream of it and a unique restriction enzyme site downstream, *in vitro* transcripts of the cDNA are readily synthesized. Because the

RUBV genomic RNA is of positive polarity, the *in vitro* transcript initiates infection following transfection into susceptible cells and infectious virus results. Alternatively, the structural protein ORF can be replaced with a reporter gene, such as GFP, a contruct known as a replicon (Fig 4). A replicon replicates following transfection, but cannot spread from cell to cell because it lacks the virion proteins.

In a recent study in our laboratory, bicistronic replicons were constructed that express a neomycin resistance drug-selectable marker and either GFP alone or a fusion between C and GFP (Fig. 4). Following transfection of Vero cells with these replicons, drug selection was applied to generate a cell population uniformly harboring the replicon. The cell lines containing the GFP replicon were termed IN-IN cells, and the cell line containing the C-GFP replicon were termed 925-IN cells [63]. Following initial drug selection, survival of 925-IN cells was roughly one hundred times greater than survival of IN-IN cells. Subsequent analysis of growth of these cells showed that IN-IN cells grew more slowly than Vero cells and exhibited indications of induction of apoptosis. In contrast, the 925-IN cells grew similarly to Vero cells and lacked the hallmark signs of apoptosis. The C protein's role in this striking difference in growth and survival is not yet understood. The initial belief was that C, which is known to be involved in viral RNA replication, mediated enhanced RNA synthesis and the concomitant production of the drug resistance factor. However, there was no difference between the cell lines in the amount of the subgenomic RNA synthesized from which the drug resistance factor would be translated, and Western blot confirmed that the amount of drug resistance factor was equal. The alternative hypothesis, based on previous observations that determinants of cytopathogenicity reside in the P150 gene, analyzed in this thesis is that expression of P150, alone and in the IN-IN and 925-IN replicons, is detrimental to cell growth and its binding to the capsid protein blocks this

detrimental effect. As discussed above, Vero cells are a nonhuman cell line that lacks a functional interferon system. In order to extend observations made in Vero cells to clinical relevance, human cell lines were analyzed for apoptosis induction in response to P150 in order to determine the role played by the lack of an interferon system in Vero cells with the hypothesis that these cells would undergo the same levels of apoptosis observed in Vero cells.

GOAL OF THESIS RESEARCH

1. The hypothesis that the decreased survival of IN-IN cells in comparison to Vero and 925-IN cells is due to the induction of apoptosis was tested in two ways. First, selective cell staining and fluorescent microscopy were used to measure caspase activation and chromatin fragmentation as indicators of apoptosis. Second, cells were screened using propidium iodide staining and flow cytometry to detect apoptosis as well as cell cycle perturbations.

2. The hypothesis that P150 specifically is responsible for the induction of apoptosis observed in IN-IN cells was examined by transfecting Vero cells with a plasmid expressing P150 tagged with green fluorescence protein (GFP) and utilizing the methods described above to analyze these cells for apoptosis. To test the hypothesis that the C protein can attenuate the cytopathogenicity of P150, a Vero line that was generated to constitutively express the full length rubella capsid protein was also transfected with the P150-GFP expression plasmid and was also analyzed for apoptosis using the methods described above.

3. Vero cells are an interferon-deficient line of African green monkey kidney cells. To determine if the findings in Vero cells are relevant to human cells, and concomitantly the pathogenesis of CRS, two human cells lines, A549 and HEK293 cells, were transfected with the IN-IN and 925-IN replicons with the intent to assay for apoptosis. The cytopathogenicity of P150 was also assayed by transfection with the P150-GFP expression plasmid and the methods to assay for apoptosis described previously were used.

.

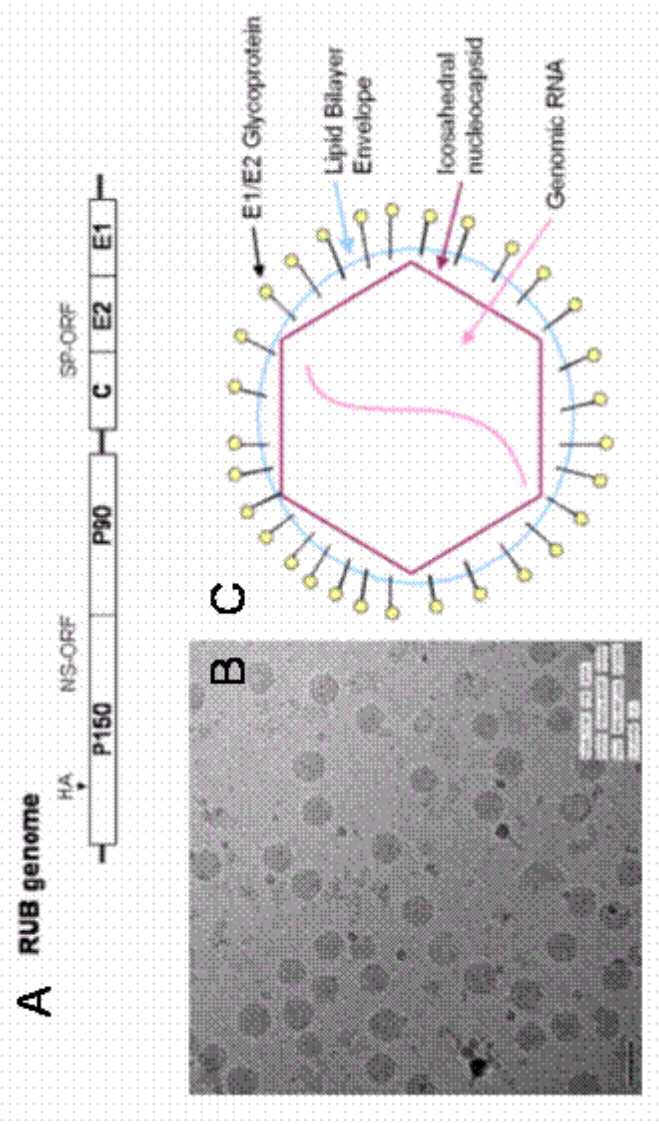

Figure 1: Schematic diagram of RUBV particle and genome. A: Diagram of RUBV genome. **B:** Electron micrograph of RUBV particles. **C:** Schematic drawing representing the structural arrangement of rubella's glycoproteins, envelope, nucleocapsid, and genomic RNA.

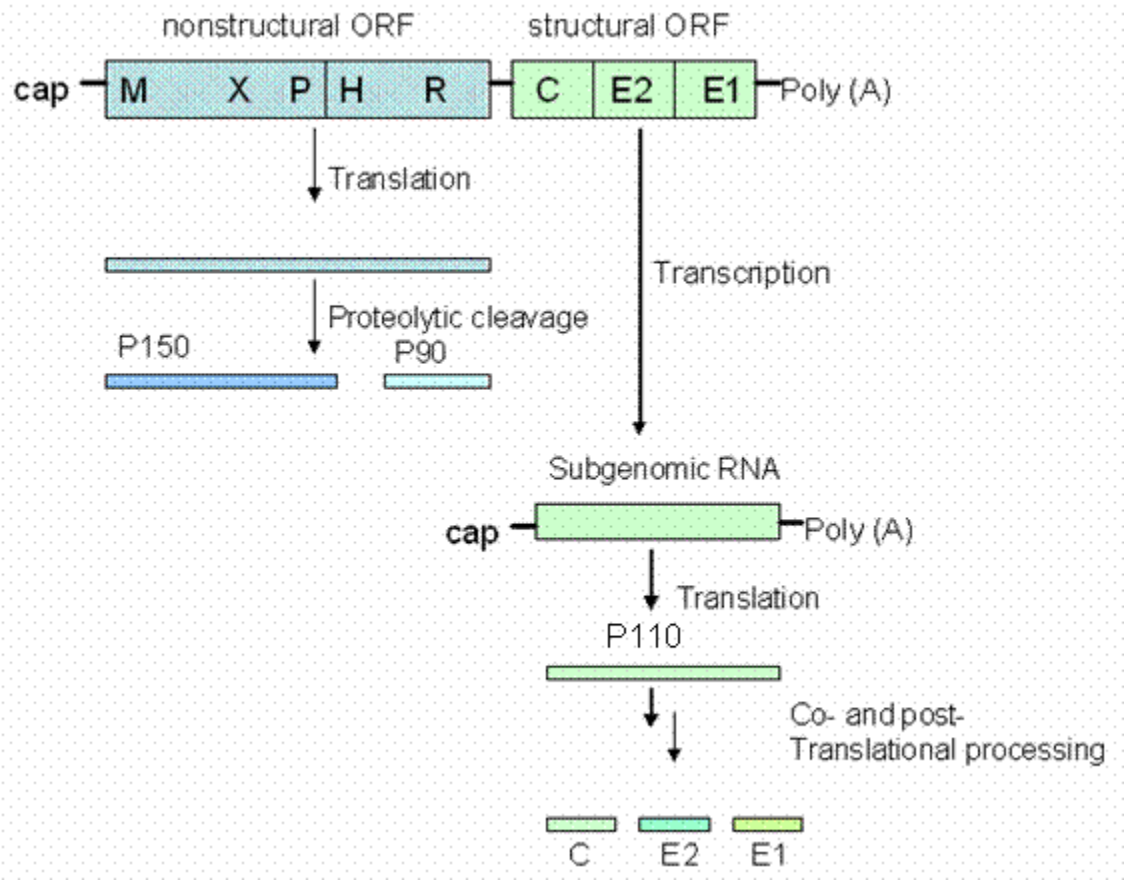

Figure 2: Schematic diagram of Rubella genome and replication scheme. The large boxes are schematic representations of the RUBV genomic and subgenomic RNA's with open reading frames denoted by boxes and untranslated regions by lines. The separate genes with the ORF's are separated by vertical lines. Thinner boxes are indicative of protein products produced. M: methyltransferase domain, X: function to be determined, P: protease domain, H: Helicase domain, R: replicase domain are motifs within the P150 and P90 replicase proteins.

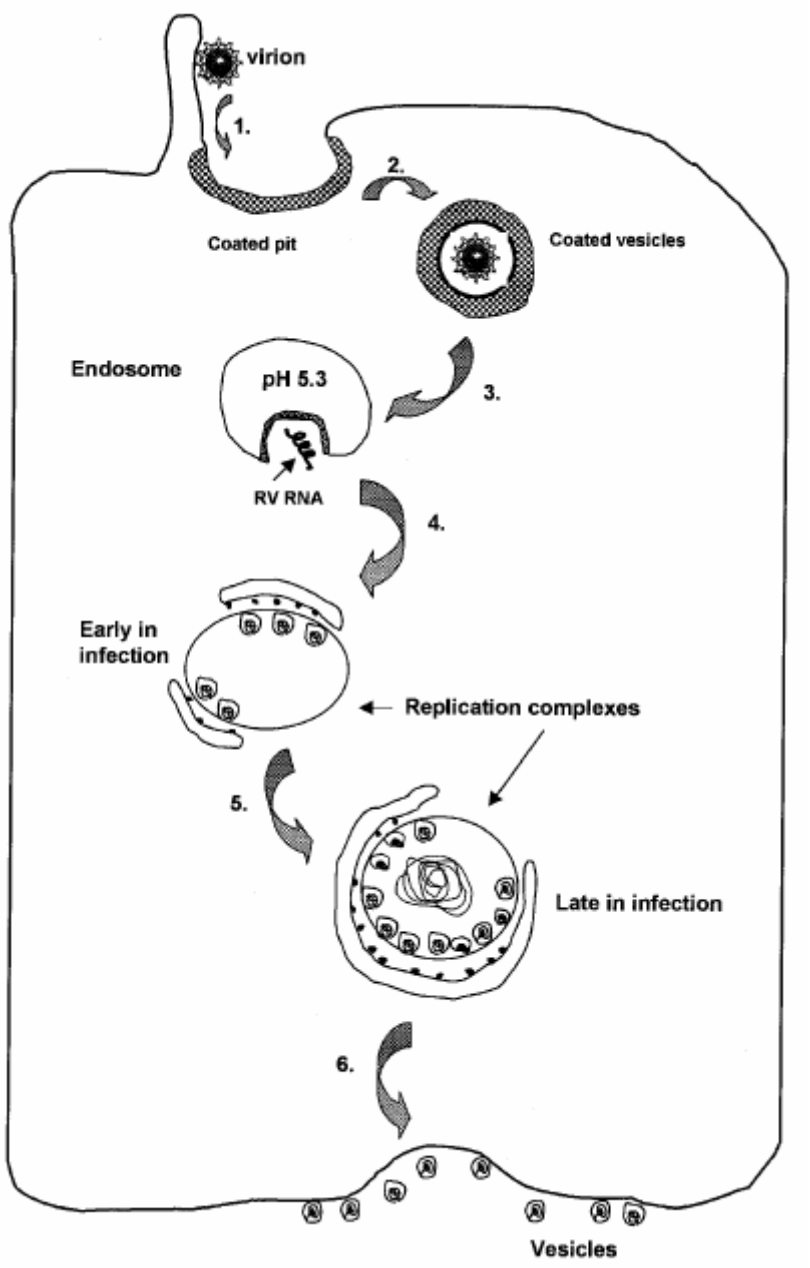

Figure 3: Schematic of Rubella replication cycle. Artistic interpretation of the steps involved in RUBV replication. Referenced from Lee and Bowden 2000.

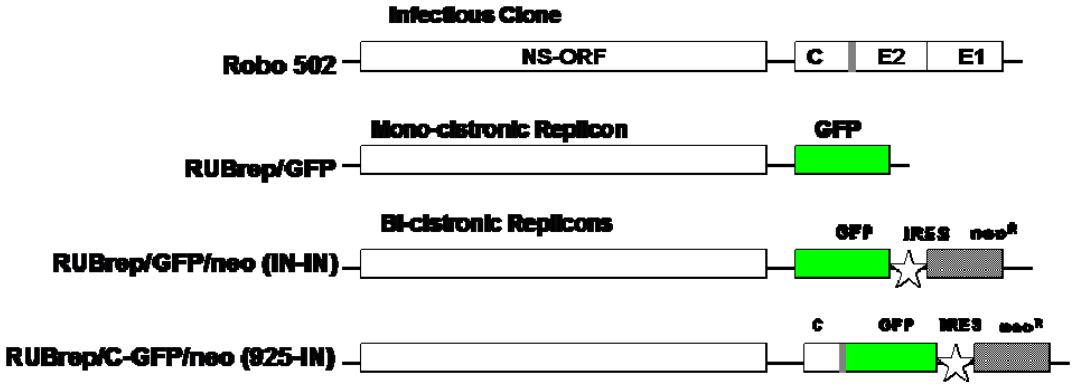

Figure 4: RUBV genome and replicons. Schematic of Robo502 RUBV infectious cDNA clone, RUBrep/GFP monocistronic replicon, IN-IN, and 925-IN bicistronic replicons.

CHAPTER II

METHODS

Cell Culture, Virus Infection, and Apoptosis Induction

The Vero (African green monkey kidney epithelial) cell line, purchased from the American Type Culture Collection (ATCC:CCL-81), was maintained at 35°C under 5% CO_2 in Dulbecco's minimal essential medium (DMEM) (Invitrogen, Carlsbad, Calif.) supplemented with 5% fetal bovine serum (FBS) and Gentamycin (10 mg/mL). The IN-IN and 925-IN cell lines, stably transfected with the corresponding replicons, as well as the C-Vero cell line which was selected for stable expression of the RUBV C protein, all provided by Dr. Wen-Pin Tzeng, were similarly maintained with the exception that the medium contained G418 Sulfate (Geneticin) antibiotic at a concentration of 100 µg/mL (Mediatech). Cells transfected with the IN-IP and 925-IP replicons were likewise maintained with the exceptions that the medium was supplemented with 10%FBS and contained Puromycin (10 ng/mL). The human cell lines HEK293 (human embryonic kidney transformed with adenovirus 5; provided by Dr Deborah Baro) and A549 (human adult lung carcinoma; ATCC:CCL-185) were maintained at 37°C under 5% CO_2 in DMEM supplemented with 10% FBS, 50 µg/mL gentamycin, 100 µg/mL penicillin, and 100 µg/mL streptomycin. All cell lines were routinely subcultured by trypsinzation.

Transfection with P150 expressing plasmids.

Two transfection reagents were used to introduce plasmids expressing either GFP or a P150-GFP fusion protein. Both plasmids were created by Dr Wen-Pin Tzeng using VR1012 (Vical, Inc., San Diego CA) as the backbone vector in which expression is controlled by the human cytomegalovirus immediate early promoter. Vero and HEK-293 cells were transfected

using Lipofectamine-2000 (GIBCO) while A549 cells were transfected using GenePORTER (Genlantis) according to manufacturer's protocol.

80% confluent cells (maintained in the appropriate supplemented DMEM) in 60mm plates were washed two times with 1 mL of phosphate buffered saline (PBS) and one time with 1 mL of Opti-MEM (Gibco/BRL). A mixture of 9 µg of plasmid and 7 µL of Lipofectamine-2000 or GenePORTER in 500 µL of Opti-MEM was then added to the cells. For mock infection a mixture of either 7 µL of Lipofectamine-200 or GenePORTER in 500 µL of Opti-MEM was added to the cells. After incubating for 24 hrs, the transfection mixture was replaced with 2 mL of the appropriate supplemented DMEM. Following transfection, GFP expression was monitored with a Zeiss Axioplan microscope with epifluorescent capability and cells were analyzed for induction of apoptosis as described below. Microscopic images were captured using Axiovision 3.1 software.

Generation of Replicon Stable Cell Lines

Cells were transfected as described above with 12 µg of *in vitro* transcripts from the following plasmids (all provided by Dr. Wen-Pin Tzeng): RUBrep-GFP-neo (IN-IN), RUBrep-CGFP-neo (925-IN), RUBrep-GFP-puro (IN-IP), or RUBrep-CGFP-puro (925-IP). Transfected cells were monitored using a Zeiss Axioplan microscope with epifluorescence capability for the expression of GFP (indicative of replicon replication). Once GFP was observed, cells were subjected to selection with the appropriate supplemented DMEM containing either 1000 µg/mL G418 or 100ng/mL puromycin to select for cells harboring the replicons. Once a homogenous

population was developed it was maintained in appropriately supplemented media containing either neomycin or puromycin.

Apoptosis assays: Vero, IN-IN, and 925-IN cells were seeded at 10^4 cells/mL in 35 mm plates and analyzed for apoptosis (see below) every 24 hours through 4 days post-seeding. Cells transfected with plasmids expressing GFP or P150-GFP were analyzed for apoptosis 48 or 72 hrs post transfection. Two positive controls were performed. Cells were infected with RUBV or treated with the PKC-inhibitor staurosporine. For infection with RUBV, cells were seeded in 35 mm plates. After the cells reached confluency, 0.5 ml of phosphate buffered saline (PBS) containing 18μL of RUBV stock (Therien strain, obtained from Yumei Zhou) were added to obtain a multiplicity of infection of 1.0 pfu/cell and the culture was incubated at 35^{o}C for 1 hour. Subsequently, the inoculum was replaced with 2mL of supplemented DMEM. In order to chemically induce apoptosis, cells were incubated for 1 hour in the presence of staurosporine (Trevigen, 0.1mM); analysis for apoptosis was performed immediately post-treatment.

Apoptosis: Activation of Caspases

Cells were stained with CaspaTag (Chemicon) 3,7-caspase fluorescent tag to test for the presence of caspase activity according to the manufacturer's protocol. Cells were seeded on sterile glass coverslips in 35 mm plates containing 2mL of the appropriate supplemented DMEM. The media was removed and cells were washed with 1mL PBS. Cells were then incubated for one hour with CaspaTag reagent under 5% CO_2. After incubation stain was removed and cells were counterstained with Hoechst stain in order to visualize nuclear

morphology. Finally cells were washed two times with 2mL wash buffer and then were analyzed. Adherent cells were analyzed by fluorescence microscopy using a Zeiss Axioplan microscope with epifluorescence capability. Cells were also suspended by trypsinization and analyzed using a BD FACSCanto flow cytometer utilizing an Argon laser counting 10,000 events. Data was compiled and analyzed using FACSDivae Software.

Apoptosis: Cell Cycle Disruptions

Cells grown in 35 mm plates were harvested through trypsinization and suspended in cold PBS. While vortexing vigorously, an equal volume of 70% ice cold ethanol was added drop wise and the suspension was incubated for no less than 30 min at 4°C. The ethanol was removed by low speed centrifugation and the cells were resuspended in cold PBS. The cells suspended in PBS were then incubated for 30 min with 50 µL RNase I (Epicenter 10 µg/mL) and 20 µL propidium iodide 1mg/mL (Sigma-Adrich) at 35°C and then analyzed by flow cytometry counting 10,000 events using a BD FACSCanto with FACSDiva software.

TUNEL assay for Apoptotic DNA Fragmentation

Chemicon's ApopTag Red TUNEL assay protocol was followed according to the manufacturer instructions. Cells grown on coverslips as described above were washed in PBS and fixed in 1% Paraformaldehyde in PBS for 10 min at room temperature and then washed twice again with PBS. Cells were then post-fixed in ice-cold 70% EtOH for 5 min at -20°C and washed with PBS. Equilibration buffer consisting of potassium cacodylate provided with the kit was applied for 10 sec and cells were incubated in reaction buffer containing digoxigenin-labeled nucleotides and terminal deoxynucleotide transferase (TdT) at 37°C for 1 hour in a humidified

chamber. Stop/Washer was applied for 10 min at room temperature and cells were washed with PBS. Rhodamine conjugated to anti-digoxigenin antibody was added and cells incubated for 30 min at room temperature in the dark. After incubation cells were counterstained with DAPI to visualize nuclei and observed with a Zeiss Axioplan microscope with epifluorescence capability. Cells were also trypsinized post-staining and the suspension was then analyzed by flow cytometry counting 10,000 events using a BD FACSCanto with FACSDiva software.

CHAPTER III

RESULTS

Analysis of cell cycle and apoptosis in IN-IN and 925-IN cells

Induction of caspase-dependent apoptosis in IN-IN cells

In order to determine whether the attenuated growth exhibited by IN-IN cells was due to the induction of apoptosis, the activation of cellular caspases was assayed in Vero, IN-IN and 925-IN cells over a time period of four days post-seeding using a substrate-specific fluorescent marker for activated effector caspases 3 and 7. It was found that caspases were activated in IN-IN cells, but not in either Vero or 925-IN cells to a detectable degree. Over the growth cycle, Vero cells continued to grow until reaching confluency with only minimal caspase activation that could be attributed to natural cell number maintenance (Figure 5A: A-D). Like Vero cells, 925-IN cells grew to confluency with only a perceived natural level of caspase activation (Figure 5A: E-H). However, the IN-IN cells showed multiple anomalies compared to these other two cell lines (Figure 5A: I-L). Firstly, IN-IN cells never reached confluency and cell numbers appeared to decline over the four-day growth curve. Secondly, these cells appeared to be almost double the size of either Vero or 925-IN cells. Finally, IN-IN cells exhibited activation of caspases in addition to other morphological hallmarks of apoptosis such as membrane blebbing and chromatin condensation within the nucleus. When quantified, 40-60% of the cells exhibited caspase activation on each day of the experiment (Fig. 5B).

Cell cycle disruption in IN-IN cells

As a second assay to detect apoptosis through the observation of a sub-G_0 hump, FACS of propidium iodide-stained cells was used to measure DNA content in individual Vero, 925-IN and IN-IN cells harvested daily over a 4 day growth curve. Vero and 925-IN cells showed an almost identical progression of the cell cycle (Figure 6) with the characteristic prominent peak representative of the G_0/G_1 phase of the cell cycle as well as a smaller peak of twice the fluorescence intensity representative of G_2 and cells in between these peaks in S phase. Gradually, cells in S phase disappeared as the cells reached confluency with a G_1/G_0 peak and a small G_2 peak remaining. IN-IN cells did not exhibit a pattern matching this norm in that the G_2 peak was much larger than the G_0/G_1 peak , indicating that these cells had stalled in G_2 and were unable to proceed through the rest of the cell cycle and divide appropriately. An additional point of interest was that on day 1, cells with a DNA content greater than G_2 phase were present, suggesting that some of the cells had become tetraploid and were proceeding into the cell cycle as tetraploids. However, the proportion of such cells decreases on days 2 and 3 and the population disappeared on day 4. No cells with a sub-G_0/G_1 DNA content, characteristic of apoptosis, were observed. However, in a previous study we found that cells detach from the monolayer ("floaters") and are lost in this assay [21].

Chromatin fragmentation in IN-IN cells

Because the fragmentation of nuclear chromatin is one of the earliest hallmarks of apoptosis to manifest, a TUNEL assay was used to determine the extent to which fragmentation was occurring in Vero, 925-IN, and IN-IN cells. This was quantified by FACS as shown in Fig. 7. Once again, 925-IN cells exhibited little to no fragmentation above what was observable in

normal Vero cells. IN-IN cells immediately exhibited elevated fragmentation on day 1 post-seeding, approximately twice what was seen in 925-IN and Vero cells. This trend became even more pronounced by 2 days in IN-IN cells showing almost eight times as much fragmentation as 925-IN cells, correlating with the level of caspase activation that is observable at this time point also. Interestingly, days three and four demonstrated a decrease in the level of chromatin fragmentation in IN-IN cells to a point that is only somewhat higher than what was observed on day 1 for these cells.

Analysis of toxic effects of P150 and inhibition of toxicity in the presence of C

Induction of caspase-dependent apoptosis in Vero cells

To test the hypothesis favored by the lab that P150 is the moiety responsible for RUBV apoptotic affects in Vero cells, including IN-IN cultures, Vero cells were mock-transfected or transfected with a plasmid expressing GFP or a P150-GFP fusion protein. By 48 hours post-transfection, toxic effects of the P150-GFP expressing plasmid could be seen microscopically in Vero cells such as dramatic decreases in cell number, rounding of cells, and the appearance of floaters in the medium (data not shown). To determine if apoptosis was behind the observed toxicity, cells were then stained with a substrate-specific fluorescent marker for activated effector caspases 3 and 7 (CaspaTag). As shown in Fig. 8A, every cell that harbored the plasmid containing P150-GFP (fluorescing green) was also observed to have activated caspases, and thus was undergoing apoptosis while their counterparts in the GFP-plasmid transfected culture showed no detectable activation of caspases. Quantitation by FACS revealed that ~80% of the

P150-GFP transfected cells exhibited caspase activation vs ~10% of the GFP transfected cells (Fig. 8B).

Having proven that P150 does in fact induce apoptosis in Vero cells, the second part of the hypothesis needed to be tested, namely that C neutralized the toxic effects of P150 (possibly through its interaction with P150). In order to do this, a cell line that stably produces RUBV C protein that was previously established in our lab (termed C-Vero cells) was transfected with the P150-GFP plasmid. At 48 hours post-transfection, C-Vero cells exhibited none of the cytopathic effect observed in similarly transfected Vero cells and no evidence of apoptosis was apparent by Caspatag staining (Figure 8A and B).

Chromatin fragmentation in transfected Vero and CVero cells

As a second assay to establish the ability of P150 to cause the induction of apoptosis in Vero cells, the fragmentation of cellular DNA was investigated using a TUNEL assay. Vero cells transfected with the P150-GFP plasmid and stained 48 hours post-transfection exhibited marked DNA fragmentation (Figure 9 A and B) while mock-transfected and GFP plasmid transfected Vero cells showed no DNA fragmentation at all further establishing the toxic effects of P150 in Vero cells. On the other hand, CVero cells transfected with P150-GFP as well as their mock-transfected and GFP-plasmid transfected counterparts showed no fragmentation of the chromatin that was detectable.

Effects of P150 on the cell cycle

The previous two assays established that P150 induces apoptosis in Vero cells independently of any other viral proteins. Next, the effects it may have on the cell cycle were determined. Contrary to the dramatic effects of the IN-IN replicon on the cell cycle, there appeared to be no effect at all in Vero cells transfected with P150-GFP (Figure 10C). In fact, comparison of these cells to mock-transfected (Fig. 10A) or GFP-transfected (Fig. 10B) cells showed no fundamental change in the pattern produced. When C-Vero cells were transfected with P150-GFP, they too showed no ill effects on the progression of the cell cycle (Figure 10F). In fact, these cells showed identical cell cycle patterns to mock-transfected (Fig 10D) and GFP-transfected (Fig. 10E) C-Vero cells as well as mock-transfected and GFP-transfected Vero cells. Given that P150-GFP did not affect the cell cycle in Vero cells and P150-GFP induction of apoptosis was inhibited in C-Vero cells, it was expected that P150-GFP-transfected C-Vero cells would exhibit no abnormalities in their progression through the cell cycle.

Introduction of Replicons into Human Cell Lines

Two human cell lines, HEK293 and A549, were transfected with the 925-IN and IN-IN replicons in order to ascertain if the lack of a functional interferon system played a critical role in the replication of the replicons in transfected cells. Due to an apparent natural immunity to the drug neomycin exhibited by these cell lines, an alternate replicon was obtained from Dr Wen-Pin Tzeng, 925-IP and IN-IP, in which the neomycin resistance marker was replaced with a puromycin resistance marker. Cells were monitored post-transfection through fluorescent microscopy for the presence of GFP. Approximately 24 hrs post-transfection GFP was detected and 10 ng/mL puromycin was added to the medium in order to select for cells harboring the

replicons. Approximately one week post-transfection, GFP was more difficult to detect in the cultures. Two weeks post-transfection no GFP could be detected and all the cells in the culture died within three weeks. Because a stable line harboring either replicon could never be established, experiments could never be conducted in an identical manner to Vero cells.

Analysis of P150 induction of apoptosis in human cells

Caspase activation in transfected HEK293 and A549 cells

Although establishment of stably transfected human cells lines with the IN-IP and 925-IP replicons was not successful, to see if P150 induces apoptosis in either HEK293 or A549 cells, both were transfected with the P150-GFP-expressing plasmid and caspase activation was measured 48 hrs post-transfection. As shown in Fig. 10, the transfection efficiency of HEK 293 cells was much higher than of A549 cells. In both cell lines, number of caspase positive cells in GFP-transfected cells was similar to the mock-transfected control. However, in the P150-GFP-transfected cultures, there was a marked increase in the number of cells with activated caspases (Figs 10A, panels C and F), these caspase-positive cells did not overlap or correlate with cells that fluoresces green and actually harbors the plasmid expressing P150-GFP. Rather the caspase-activated cells in the cell culture surrounded the successfully transfected (green) cells. This observation was borne out by FACS analysis (Fig. 10B) which revealed no increase in caspase activation among P150-transfected cells in either cell line.

Chromatin fragmentation in P150-transfected human cells

As a second assay to confirm the apparent lack of apoptosis induced by P150 in the human HEK293 and A549 cells, these cells were transfected with GFP- or P150-GFP-plasmids

and examined 48 hours post-transfection by TUNEL assay for the DNA fragmentation. Both microscopically (Fig. 13A) and by FACS (Fig. 13B), in both cell lines, cells expressing GFP or P150-GFP and cells exhibiting chromatin fragmentation did not overlap, indicating that P150 did not induce chromatin fragmentation in either cell line. Unlike the caspase activation assay, there was not an apparent increase in apoptotic cells in the P150-GFP-transfected cultures and thus that observation is unexplained.

Effects of P150 on the cell cycle progression in human cells

HEK293 and A549 cells were transfected with GFP or P150-GFP-plasmids were stained 48 hours post-transfection with propidium iodide and analyzed by FACS. FACS gating was adjusted so that propidium iodide staining was quantified in successfully transfected (ie; green) cells (Figure 12). Compared with the control population which is quiescent in A549 cells, cells transfected with P150-GFP showed an increase in the number of cells in G2 while GFP transfected cells mirrored the control population. Conversely, the GFP-transfected HEK cells showed an increase in cells in G2 compared with P150-GFP transfected cells. Thus, there was no consistent compelling alterations of the cell cycle induced by P150 in these two cell lines.

Figure 5: Analysis of caspase-dependent apoptosis in Vero, 925-IN and IN-IN cells A: Vero cells (panels A-D), 925-IN cells (panels E-H), and IN-IN cells (panels I-L) were seeded at a concentration of 10^4 cells/mL and allowed to grow for 1 (panels A, E, and I), 2 (panels B, F, and J), 3 (panels C, G, and K), or 4 (panels D, H, and L) days. Cells were then co-stained with CaspaTag caspase-3,7 fluorescent marker (red) and Hoechst (blue) and observed under a fluorescence microscope. The green color is due to expression of a C-GFP fusion protein by 925-IN cells and GFP by IN-IN cells. In comparison with Vero and 925-IN cells, IN-IN cells exhibited decreased cell density, increased size, caspase induction, blebbing of the cytoplasmic membrane, and chromatin condensation (the latter two are indicated by arrows in Panels I and J, respectively. **B:**The percentage of Vero, IN-IN, and 925-IN cells exhibiting caspase activation was quantitated by FACS. The results are the mean of 4 independent experiments; the error bars represent the standard error of the mean.

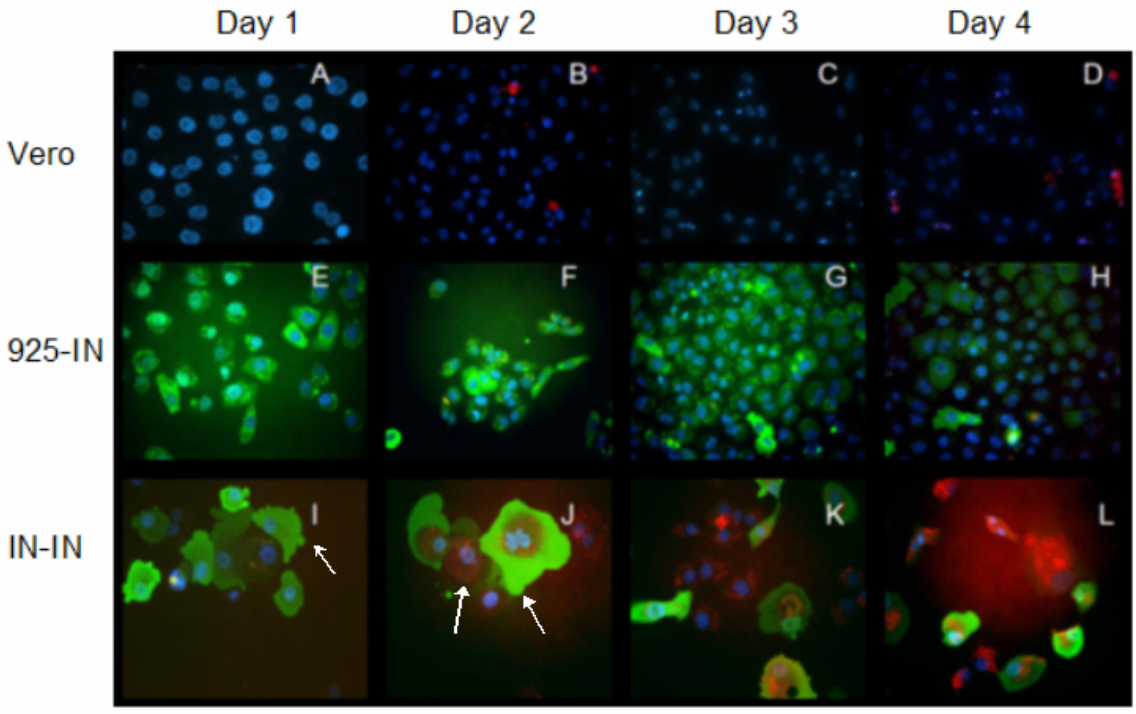

Figure 5A

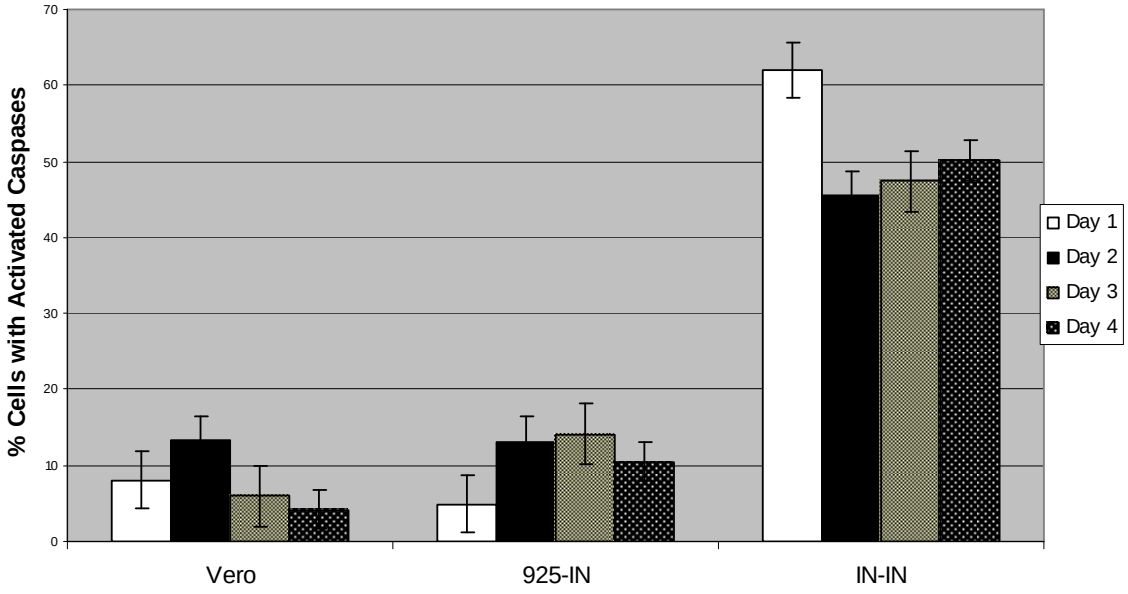
% Cells with Activated Caspases
70
60
50
40
30
20
10
0
Vero
925-IN
IN-IN
Day 1
Day 2
Day 3
Day 4

Figure 5B

Figure 6: Cell cycle analysis of Vero cells, 925-IN, and IN-IN cells Vero cells (panels A, D, G, and J), 925-IN cells (panels B, E, H, and K), and IN-IN cells (panels C, F, I, and L) were seeded at a concentration of 10^4 cells/mL and grown for 1 (panels A, B, and C), 2 (panels D, E, and F), 3 (panels G, H, and I), or 4 (panels J, K, and L) days. Cells were stained with propidium iodide and analyzed by FACS. Cell count on the Y-axis is plotted as a function of PI staining on the X-axis. The peaks of cells in the G0/G1 and G2 stages of the cell cycle are indicated.

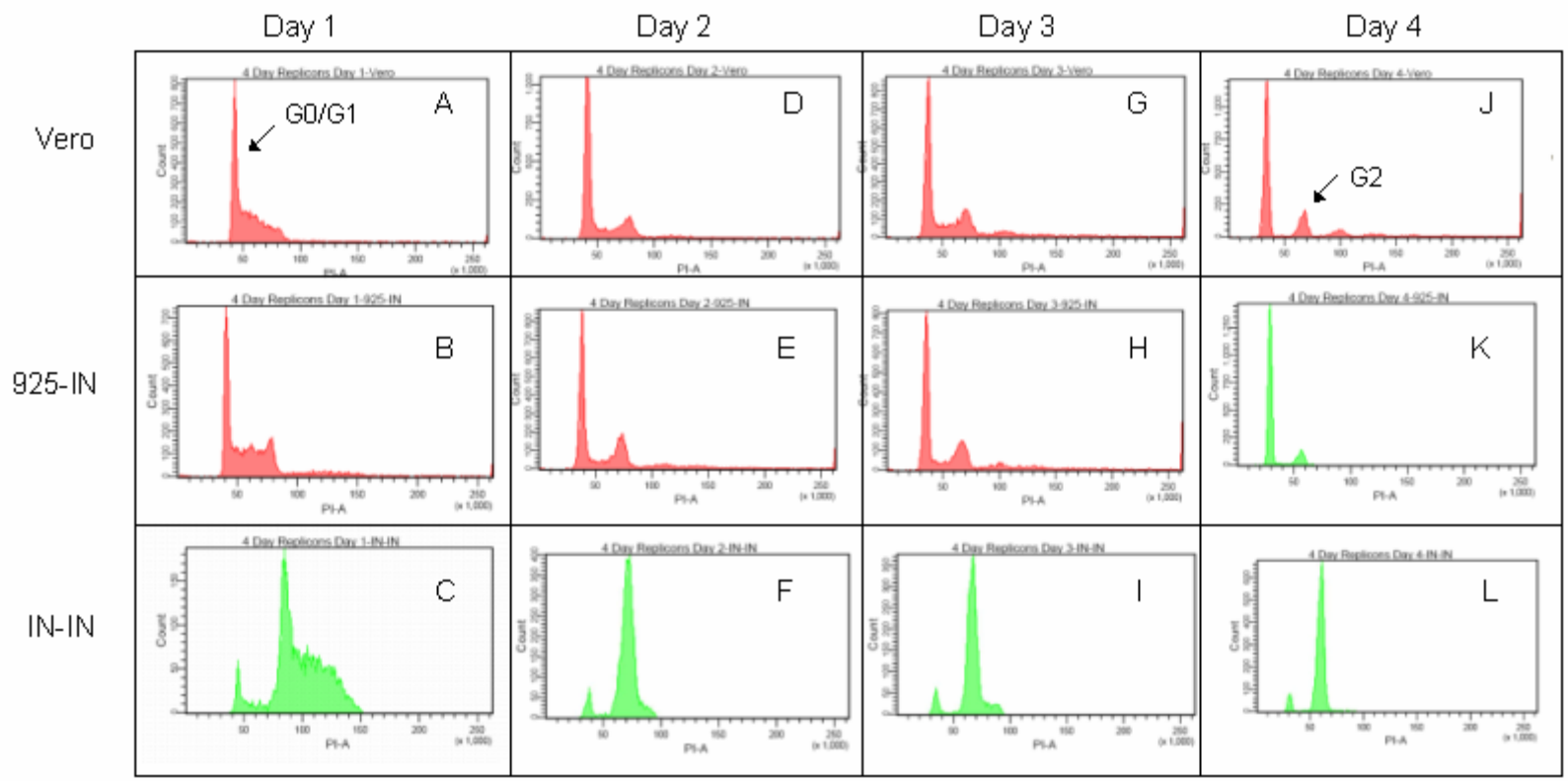
Day 1
Day 2
Day 3
Day 4
Vero
925-IN
IN-IN
A
B
C
D
E
F
G
H
I
J
K
L
G0/G1
G2

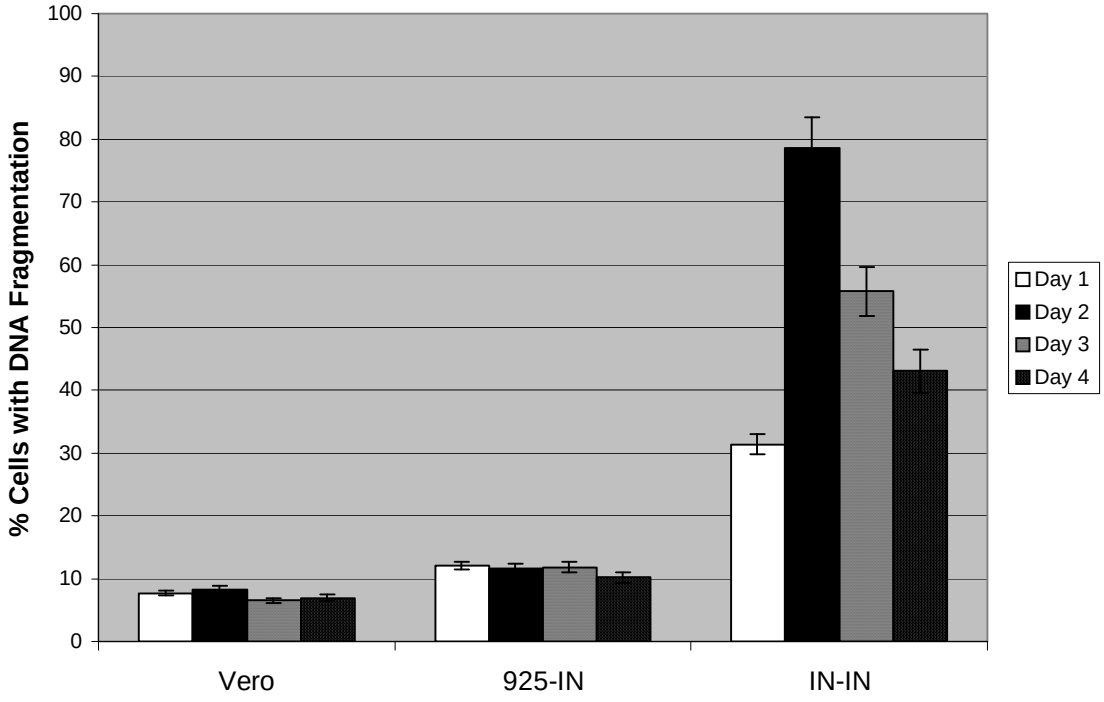

Figure 7: Chromatin fragmentation as an assay for apoptosis in Vero, 925-IN, and IN-IN cells. Vero cells, 925-IN cells, and IN-IN cells were seeded at a concentration of 10^4 cells/mL and grown for 1, 2 , 3, or 4 days. Fluorescent DNA end labeling (TUNEL), assayed by FACS for individual cells, was used to detect chromatin fragmentation. The results are the mean of 4 independent experiments; the error bars represent the standard error of the mean

Figure 8: Analysis of caspase-dependent apoptosis in Vero and CVero cells transfected with P150. A: Vero cells (panels A-C) and C-Vero cells (panels D-F) were mock-transfected (Panels A and D), transfected with a plasmid expressing GFP (Panels B and E) or a P150-GFP fusion protein (Panels C and F). At 2 days post-transfection, cells were co-stained with CaspaTag (Chemicon) activated caspase-3,7 marker (red) and Hoechst (Chemicon) DNA marker to delineate nuclei (blue). **B:** The percentage of GFP-positive cells in the GFP and P150-GFP-transfected Vero and C-Vero cell cultures exhibiting caspase activation was quantitated by FACS. The results are the mean of 4 independent experiments; the error bars represent the standard error of the mean.

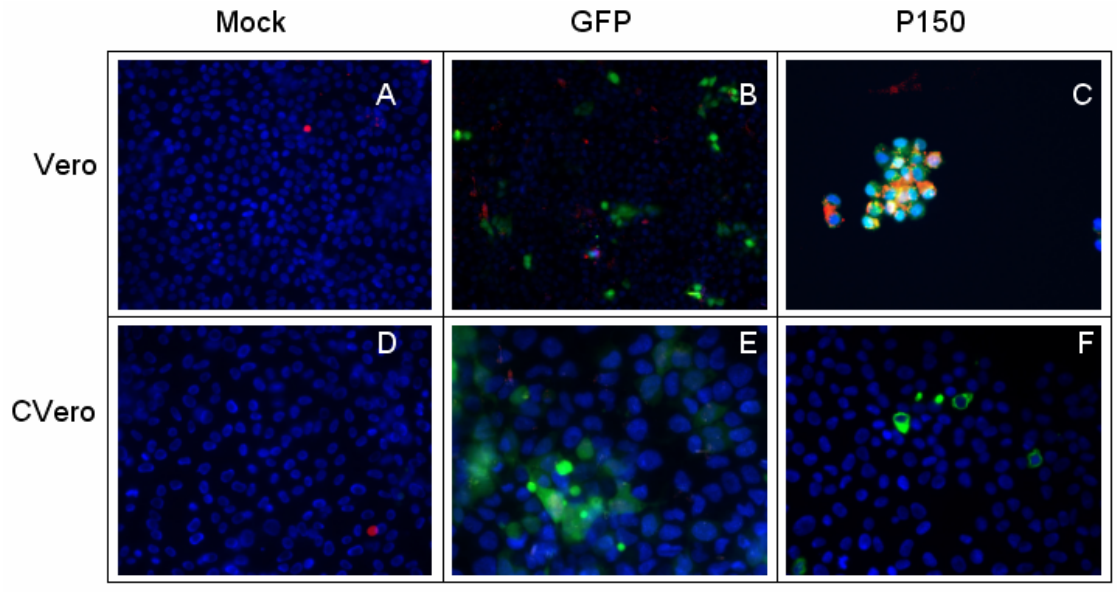

Figure 8A

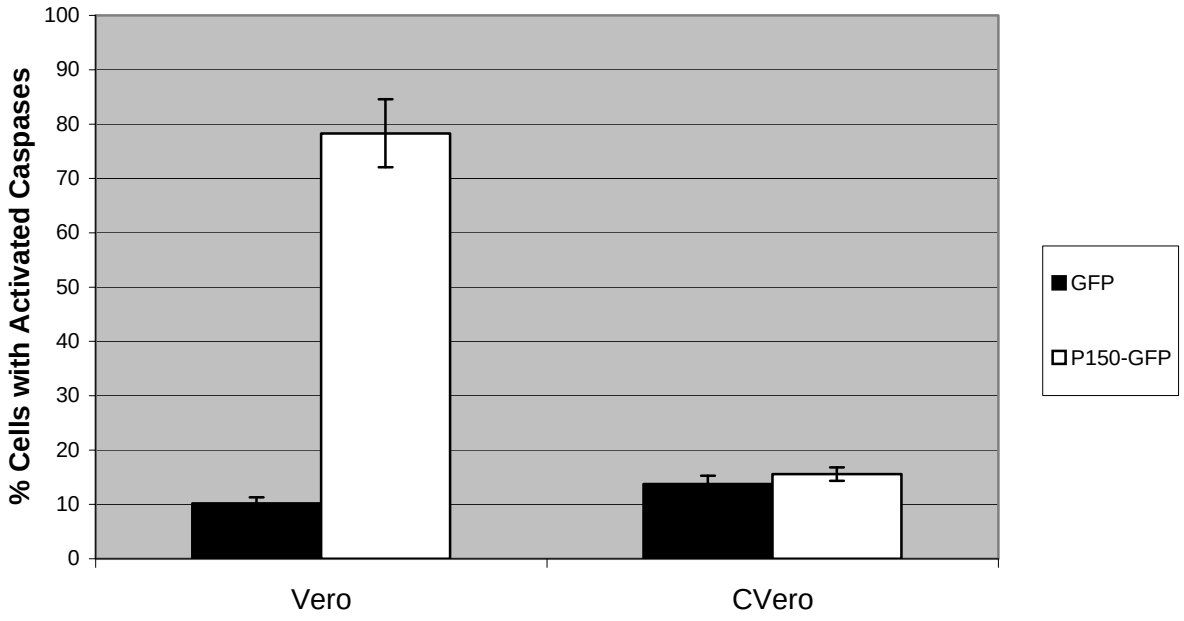
% Cells with Activated Caspases
100
90
80
70
60
50
40
30
20
10
0
Vero
CVero
GFP
P150-GFP

Figure 8B

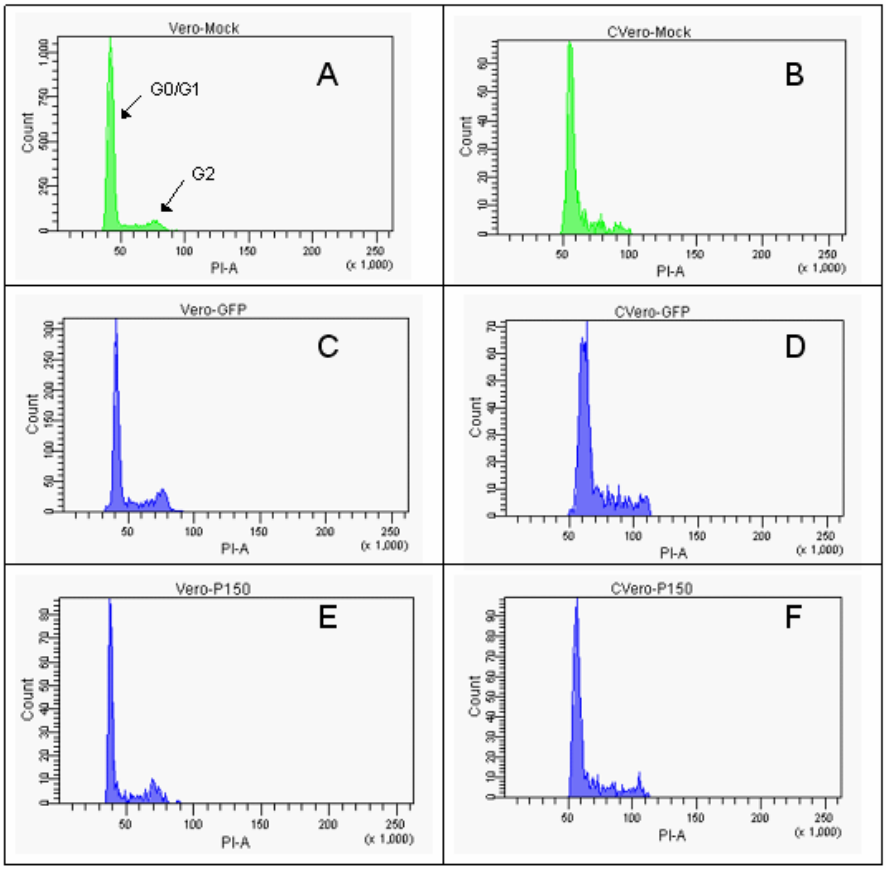

Figure 9: Cell cycle analysis of Vero and C-Vero cells transfected with P150. Vero cells (Panels A, C, and E) and C-Vero cells (Panels B, D, and F) were mock-transfected (Panels A and B) or transfected with plasmids expressing GFP (Panels C and D) or a P150-GFP fusion protein (Panels E and F). Approximately 48 hours post-transfection cells were stained with propidium iodide and analyzed by FACS. Cell count on the Y-axis is plotted as a function of PI staining on the X-axis. The total mock-transfected cell population is shown as a control while the GFP and P150-GFP-transfected populations were gated to include only GFP-positive cells. The peaks of cells in the G0/G1 and G2 stages of the cell cycle are indicated.

Figure 10: Induction of apoptosis in Vero and CVero cells by P150 detected by TUNEL

A:. Vero cells (panels A-C) and C-Vero cells (panels D-F) were mock-transfected (Panels A and D) or transfected with a plasmid expressing GFP (Panels B and E), or P150-GFP (Panels C and F). 48 hours post-transfection cells were stained by TUNEL assay (red) and counterstained with Hoechst (blue) to delineate nuclei. **B:** The percentage of GFP-positive cells in the GFP and P150-GFP-transfected Vero and C-Vero cell cultures exhibiting DNA fragmentation was quantitated by FACS. The results are the mean of 4 independent experiments; the error bars represent the standard error of the mean.

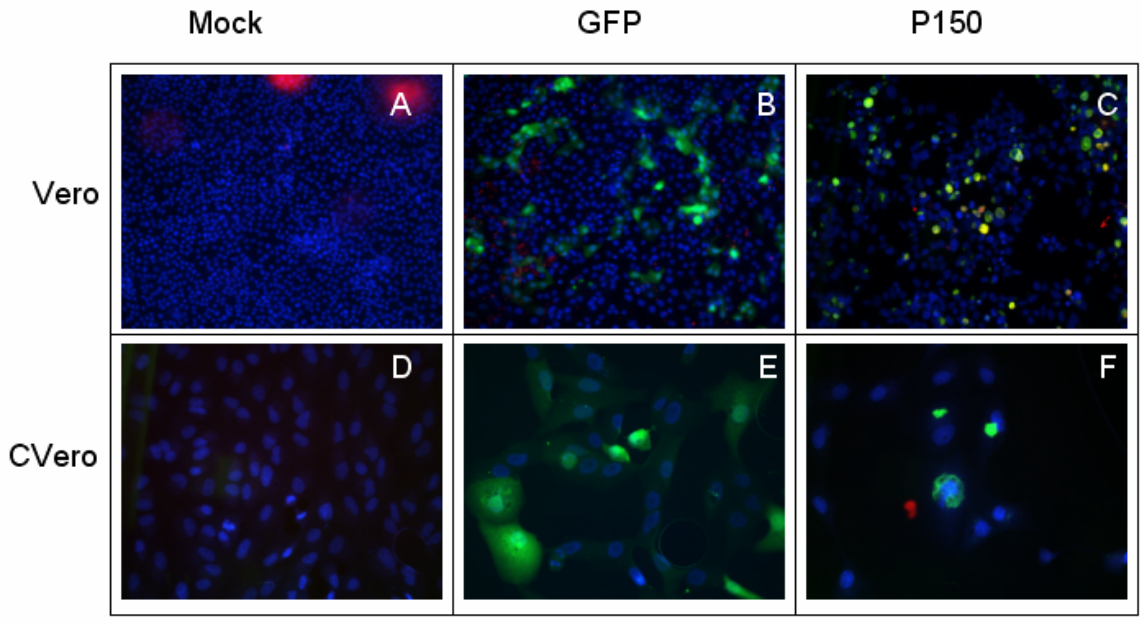

Figure 10A

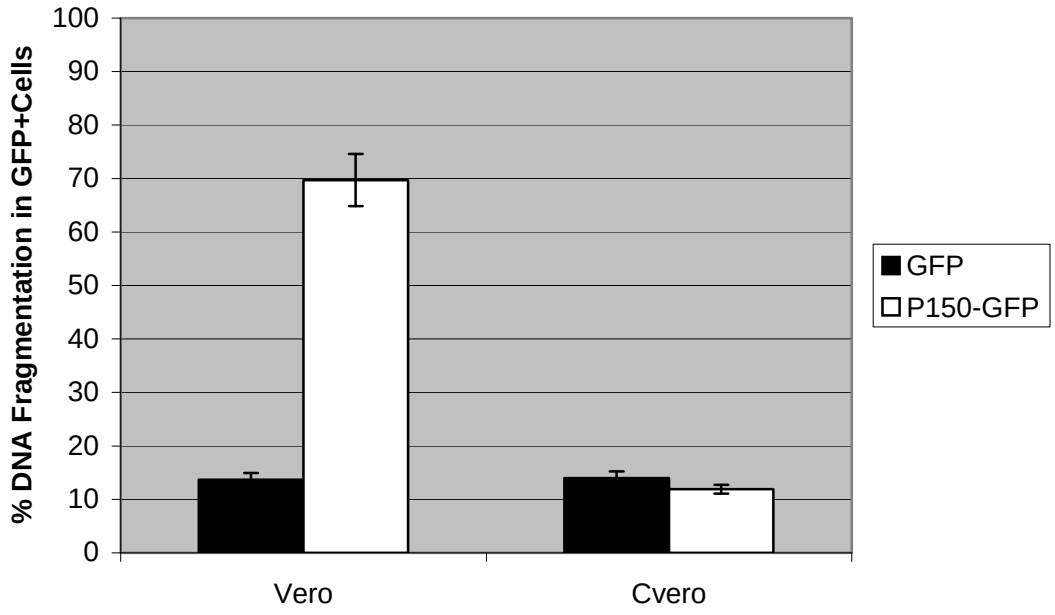
% DNA Fragmentation in GFP+Cells
100
90
80
70
60
50
40
30
20
10
0
Vero
Cvero
GFP
P150-GFP

Figure 10B

Figure 11: Caspase Analysis of caspase-dependent apoptosis in A549 & HEK293 transfected with P150. A: A549 cells (panels A-C) and HEK 293 cells (panels D-F)) were mock-transfected (Panels A and D) or transfected with plasmids expressing GFP (Panels B and E) or P150-GFP (Panels C and E) Three days post-transfection cells were co-stained with CaspaTag to detect activated caspases (red) and Hoechst (blue) to delineate nuclei and analyzed by fluorescence microscopy **B:** The percentage of GFP-positive in the GFP and P150-GFP-transfected A549 and HEK293 cell cultures exhibiting caspase activation was quantitated by FACS. The results are the mean of 4 independent experiments; the error bars represent the standard error of the mean.

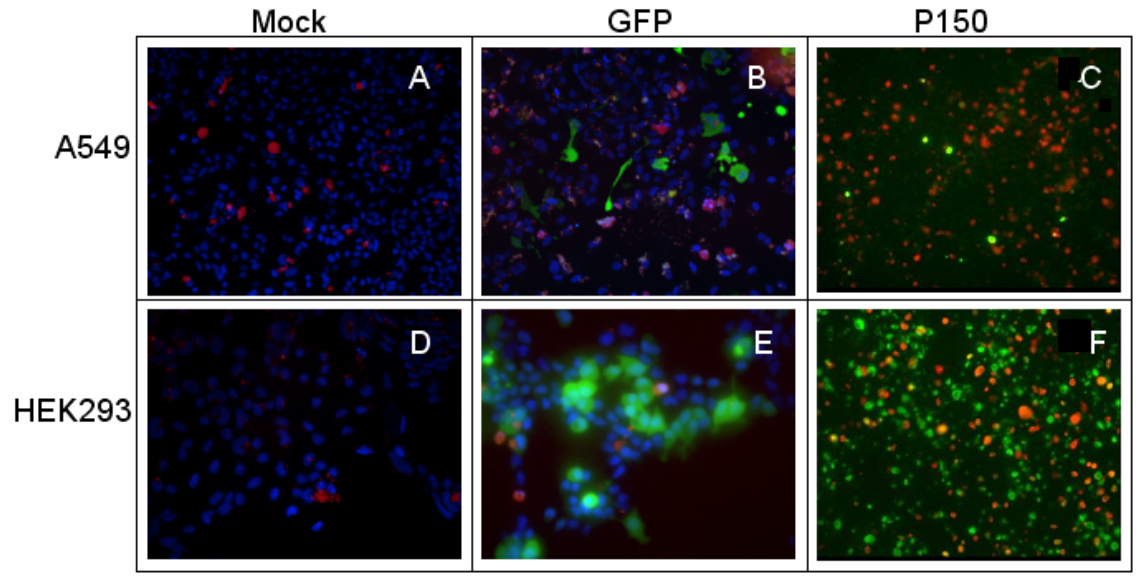

Figure 11A

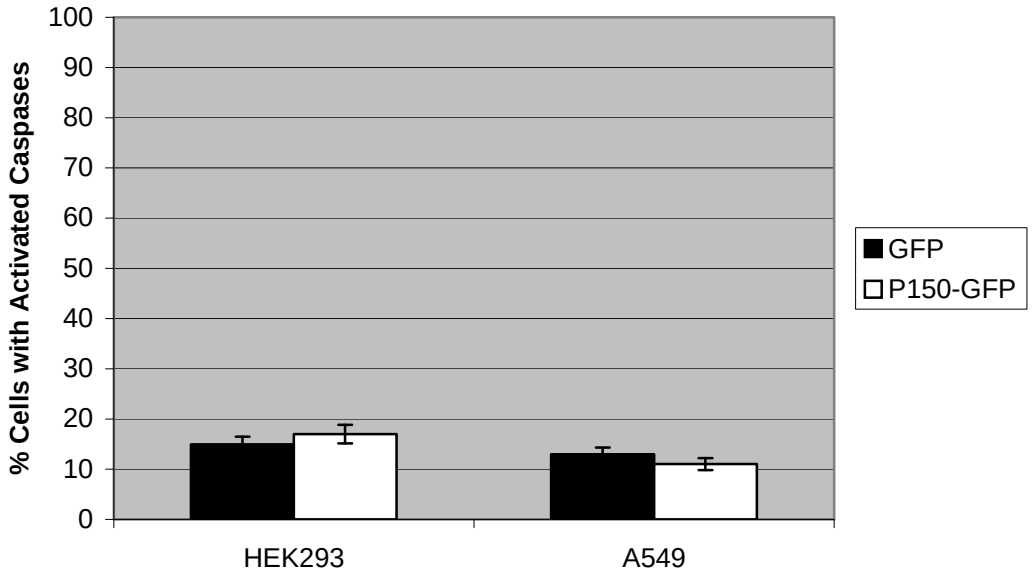
% Cells with Activated Caspases
100
90
80
70
60
50
40
30
20
10
0
HEK293
A549
GFP
P150-GFP

Figure 11B

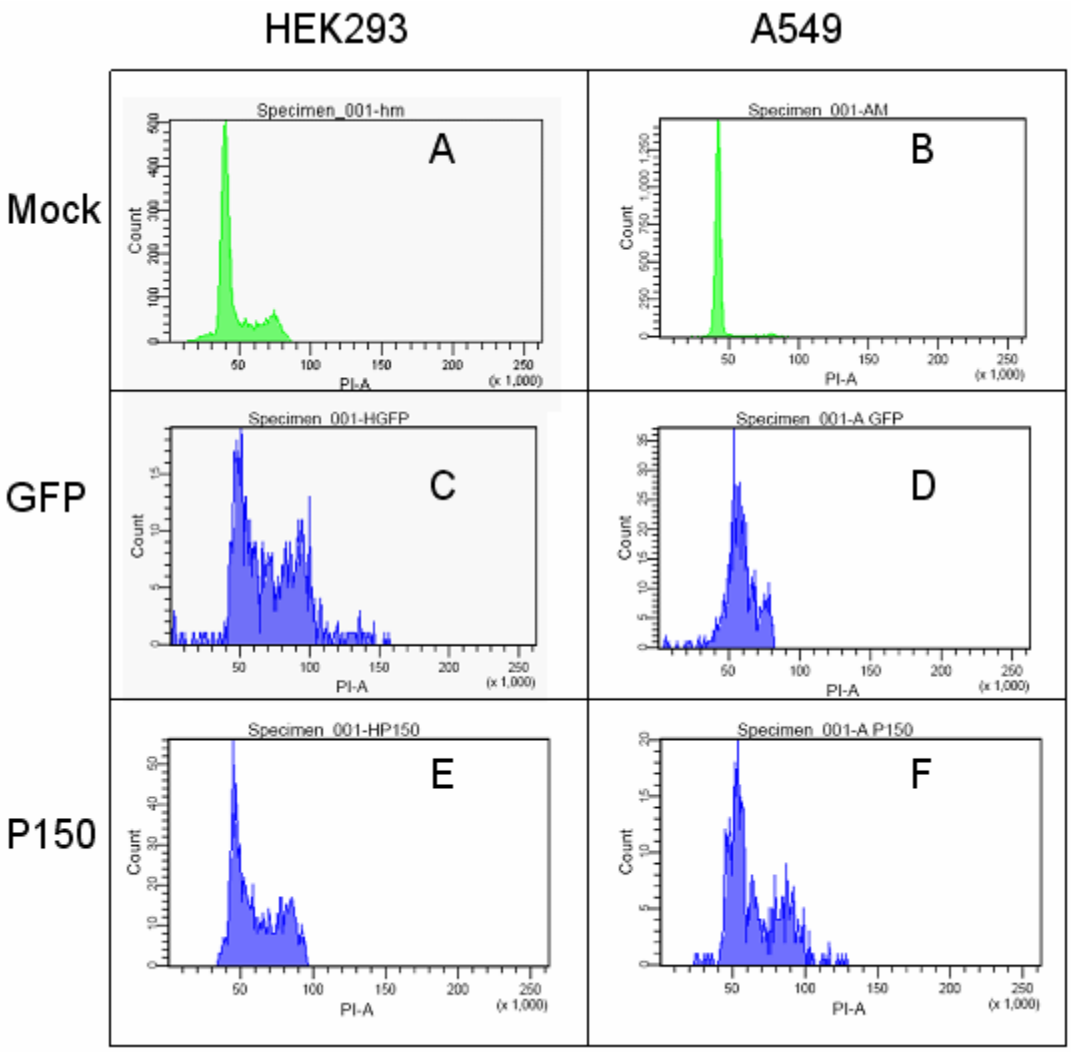

Figure 12: Cell cycle analysis of A549 & HEK293 transfected with P150. A549 cells (Panels, B, D, and F) and HEK293 cells (Panels A, C, and E) were mock-transfected (Panels A and B) or transfected with GFP (C and D) or P150-GFP (E and F) expressing plasmids. Two days post-transfection cells were stained with propidium iodide and analyzed by FACS. Total cell populations are shown in mock-transfected cells in Panels A and B while the populations in C-F were gated to include only successfully transfected cells

Figure 13: Induction of apoptosis in A549 & HEK293 cells transfected with P150 detected by TUNEL A: A549 cells (panels A-C) and HEK293 cells (panels D-F) were mock-transfected (Panels A and D) or transfected with a plasmid expressing GFP (Panels B and E), or P150-GFP (Panels C and F. 48 hours post-transfection cells were stained by TUNEL assay (red) and counterstained with Hoechst (blue) to delineate nuclei. **B:** The percentage of GFP positive (successfully transfected) GFP- and P150-GFP-transfected A549 and HEK cells exhibiting caspase activation was quantitated by FACS. The results are the mean of 4 independent experiments; the error bars represent the standard error of the mean.

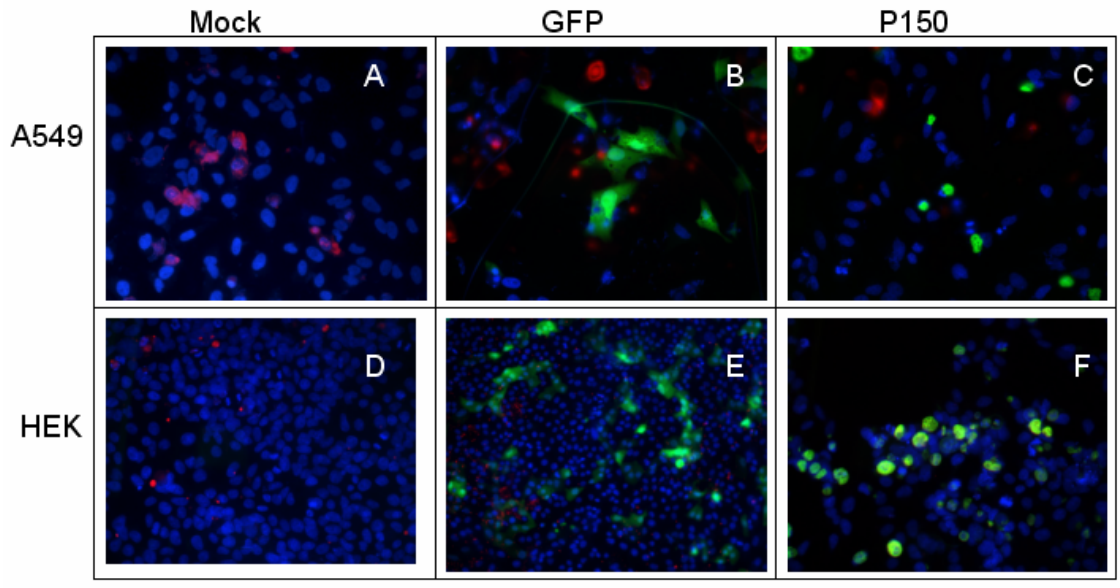

Figure 13A

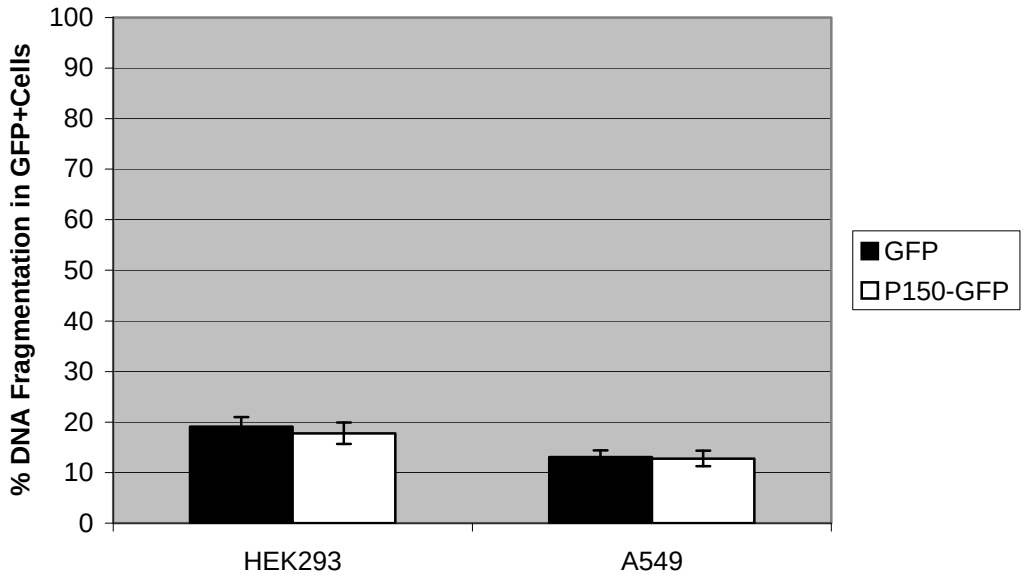
% DNA Fragmentation in GFP+Cells
100
90
80
70
60
50
40
30
20
10
0
HEK293
A549
GFP
P150-GFP

Figure 13B

CHAPTER IV

DISCUSSION

Through the existence and use of vaccines against RUBV, the disease has been restricted in most developed countries of the world. However, this virus continues to infect people annually at an unabated rate in developing countries. How rubella is able to induce complications such as arthritis and encephalitis is still unknown, and is one of the reasons this virus warrants and needs continued study. However, arguably the most important reason to continue probing the inner molecular workings of RUBV is to work towards the eventual understanding of how exactly rubella causes CRS, and with this information possibly elucidate the mechanisms by which other viruses cause congenital birth defects. Each year, another infant is born with CRS related abnormalities such as mental retardation, deafness, and cataracts. Once it is known how rubella causes CRS it might be possible to develop strategies to prevent the spread of the virus from mother to fetus or to devise prenatal treatments that would prevent the virus from infecting and damaging multiple organ systems of the fetus.

The purpose of this study was to more closely examine one proposed cause of CRS: the detrimental apoptotic effect of RUBV on the host cell. The hypothesis tested was that the RUBV non-structural replicase protein P150 induces apoptosis in the cell, both in the context of the transfected replicons and when expressed alone, and that the presence of the RUBV capsid protein neutralizes this apoptotic effect either alone or within the 925-IN replicon.

The effects of RUBV on the host cell were examined multiple ways, the first being the use of Vero cells transfected with bicistronic, drug-selectable replicons containing the RUBV non-structural ORF, the neomycin resistance gene, and either a GFP reporter gene (IN-IN) or a

C-GFP in-frame fusion reporter gene (925-IN). The ability to establish a stable cell line uniformly harboring these replicons lent an almost complete homogeneity within the population that could not be duplicated in other experiments. These cell lines also provided the first evidence that C might play a regulatory role aiding in cell survival in that cells transfected with 925-IN survived drug selection almost 10 times better than did cells transfected with IN-IN and the subsequent IN-IN cell line grew much slower than did 925-IN cells (in fact, the IN-IN cells could only be maintained by subculturing at a low dilution). These results suggested C, the only gene difference between the two replicons, plays a substantial role in aiding host cell growth and survival. This would allow RUBV more time to replicate, assemble and bud from inside the host before the cell dies.

The route through which C aids cell survival appears to be its ability to inhibit apoptosis in Vero cells. While 925-IN cells, which have C fused with GFP, grew normally and were not observed to show any indications of an abnormal level of apoptosis, within 24 hours of seeding the cells, IN-IN cells exhibited two of the earliest steps in apoptosis: the activation of caspases and chromatin condensation within the nucleus. Additionally, 24 hours after seeding, IN-IN cells exhibited apparent cytoplasmic membrane blebbing and were substantially larger than 925-IN and Vero cells. Despite the fact that there are regulatory mechanisms in the cell to halt improperly induced apoptosis, IN-IN cells seem unable to achieve this at a perceptibly efficient rate. Rather, 24 hours after the activation of caspases can be observed cells experience blebbing of the plasma membrane, and cell debris was observed 24 hours later.

Because one of the first steps in apoptosis is fragmentation of the nuclear DNA, a TUNEL assay was also used to assess the level of DNA fragmentation that had occurred in IN-IN cells. As was expected from the level of apoptosis previously observed through a caspase

activation assay, IN-IN cells demonstrated a significant level of chromatin fragmentation that both Vero and 925-IN cells lacked. This fragmentation was observed as early as one day after cells were seeded, which correlates with the time frame at which caspase activation was observed, to high levels at 48 hours after seeding, the time when chromatin condensation was observed. Fragmentation levels remained elevated through the third day post-seeding in IN-IN cells, indicating the constant apoptotic pressure to which these cells were subjected.

In addition to aiding cell survival, C also appears to play a role in cell cycle regulation and progression. FACS analysis of propidium iodide stained cells demonstrated that IN-IN cells suffered anomalies in cell cycle progression that 925-IN cells did not experience, and thus these anomalies are tied to the sole difference between the cell lines, the presence or lack of C. These analyses were originally done to detect a sub-G0/G1 peak characteristic of apoptotic cells. However, such a peak was not observed. In a previous study on apoptosis in RUBV-infected Vero cells [21], a sub-G0/G1 peak was not observed among adherent, infected cells but was observed among the "floater" populations of cells that had detached from the monolayer. Thus, at this stage of apoptosis, Vero cells have already detached. Unexpectedly however, within 24 hours of seeding, it could be seen that while Vero and 925-IN cells both showed cells predominantly in G_0/G_1 and S phases, IN-IN cells had almost no cells in either of these phases. Instead, the predominant proportion of the population appeared to be in G_2 . In addition to stalling in G_2, IN-IN cells also had cells with up to double the fluorescent intensity of G_2 indicating up to 8N aneuploidy as a result of an inability to divide multiple times. Interestingly, 48 hours after seeding and throughout the end of the experiment the existence of 8N DNA content seemed to resolve, almost as though these cells were finally able to divide semi-appropriately or died. This resolution did not lead to recovery of the cell cycle though. IN-IN

cells continued to remain predominantly in G_2 with only a few cells managing to divide and regain G_0 phase. It should be stated that it was assumed that these cells were stalled in G2 based on the lack of apparent increase in cell numbers; this would also explain the large size of these cells. However, we could not completely rule out that the IN-IN cells had become functionally tetraploid as it has been observed that RUBV can induce tetraploidy in host cells [15, 23, 81].

These observations indicated that without the presence of C, the products of the nsORF are capable of inducing abnormally high levels of apoptosis Vero cells, inducing apoptosis very efficiently and preventing these cells from growing normally or reaching confluency through disruption of the cell cycle. These effects could possibly be germane to the RUBV replication cycle in the stages surrounding virion assembly. Prior to assembly, the C protein is unbound in the cell, and thus can interact with the non-structural proteins in order to prevent their toxic effects and allow the cell to survive well enough for the virus to replicate. However, post-assembly the C is bound as a homodimer forming the virion capsid, and thus can no longer interact with non-structural proteins to inhibit their induction of apoptosis in the host. Waiting until late in the replication cycle to induce apoptosis could be construed as a survival mechanism of the virus given that if the virus has time to fully assemble and buds from the Golgi, it could potentially then be caught up in apoptotic bodies and engulfed by neighboring cells, thus transferring itself to a new host without the immune system ever recognizing its presence in the system.

In an earlier study done by the lab, RUBV-induced cytopathogenicity in Vero cells was mapped to the P150 gene [35]. In order to determine the role P150 plays in apoptosis, this gene was transfected into Vero cells through the use of a plasmid vector expressing P150 as a fusion protein with GFP. The apoptotic effects of P150 were seen microscopically in that rounded cells

were observable in the transfected culture. Every cell that expressed P150-GFP also exhibited activated caspases and chromatin fragmentation indicating that these cells were undergoing apoptosis. This induction could be solely attributed to P150 and not either the transfection solution or GFP due to the fact that cells mock-transfected or transfected with a plasmid expressing GFP only did not show any indications of apoptosis, including activation of caspases, condensation of chromatin, or any morphological change indicative of apoptosis. With the first part of the hypothesis that P150 is capable of inducing apoptosis in Vero cells proven, the question that remained, however, was whether C could aid cell survival in the presence of such a strong apoptosis inducer. This question was answered by transfecting a Vero cell line that stably expresses C (CVero) with the plasmids containing GFP or P150-GFP. These cells showed no indications of apoptosis whether transfected with GFP alone or P150-GFP either 48 hours post-transfection or one week post-transfection (data not shown). This confirms the observations made in experiments with replicons in that without C cells exposed to P150 undergo apoptosis while those with C are saved from apoptosis, proving the second part of the hypothesis. In a previous study by the lab, it was shown that C and P150 associate in the cell. While a corollary hypothesis is that this association is necessary for C to prevent apoptosis induced by P150, the experiments done in this study neither prove nor disprove this corollary hypothesis. Also beyond the scope of this study is the explanation as to why C is such an anti-apoptotic protein in Vero cells, and yet is such a pro-apoptotic protein when expressed in RK13 cells [78]. One highly interesting commonality between the two cell lines is the necessity for C to contain its C-terminal 23 amino acid membrane association sequence (the E2 signal sequence) in order to perform either of these functions (pro- or anti-apoptotic) [78, data not shown]. One possible explanation for this could be that without being membrane-bound, as it is when containing this

signal sequence, C undergoes moderate conformational changes that slightly alter its functionality.

Interestingly, the correlating results between transfection with P150 and the IN-IN replicon on induction of apoptosis did not translate to effects on the cell cycle. Both Vero and CVero cells transfected with P150-GFP showed a normal cell cycle progression. In fact, the only noticeable difference between the two cell lines transfected with P150-GFP was a slightly higher percentage of CVero cells in G_0 phase. Obviously, P150 was not subjecting Vero cells to the same cell cycle arrest as the IN-IN replicon does in the stably transfected cells despite the clear apoptotic effects in both. The Vero cells transfected with P150-GFP were almost confluent and thus normally the majority of cells in the culture would not be undergoing cell cycles subsequent to transfection with P150 while the IN-IN cells were lightly seeded and thus the majority would enter the cell cycle. The induction of apoptosis under both conditions suggested that apoptosis was not a result of the stall in G2 phase. Whether the G2 stall in IN-IN cell was the initiator of apoptosis or an independent mechanism was not answered within the scope of this study, but should still be investigated further. Interestingly, these results are consistent with a hypothesis advanced in another study that P90, the other replicase protein is responsible for cell cycle arrest [31]. It was shown that P90 colocalizes with and binds to a cytokinesis-regulatory protein, Citron-K kinase (CK) and hypothesized in the same study that this interaction interferes with CK's normal function, and thus inhibits cells from dividing, resulting in tetraploidy [31]. Vero cell lines selected to constitutively express P90 were found to exhibit a G2 block 24 hours post-seeding (albeit 24% of the cells vs almost 100% of IN-IN cells). The association of P90 with induction of apoptosis was not addressed in that study, but it is assumed that it was not profound if stable cell lines could be established. We have likewise been able to establish P90-stable cell

Vero lines, but cannot do so with P150 because of its inherent cytotoxicity (W.P. Tzeng, unpublished results). Thus P150 may induce apoptosis while P90 interferes with the cell cycle.

As interesting as these results are, the fact that Vero cells are interferon deficient could not be ignored. Thus, investigation as to whether these observations translate into a human cell culture with an intact interferon system was pursued using adult (A549) and fetal (HEK293) epithelial cells. Unfortunately, despite their ability to support replication by RUBV these cells never accepted either the 925-IN or the IN-IN replicon for more than 72 hours, likely because the replicon was eliminated by the interferon system, as was found to occur when noncytopathic replicons were transfected into murine embryo fibroblasts with an active interferon system [82]. It therefore was impossible to determine whether they would suffer cell cycle arrest and apoptosis in the same way that Vero cells harboring these replicons did. Therefore, experimentation in human cells was limited to exploring the effects of P150 and whether it would exhibit a high level of cytotoxicity in these cells.

When P150-GFP was transfected into both human cell lines, it had a much lower level of cytotoxicity, if it was at all. In fact, A549 cells that were transfected with P150 give no indication of suffering apoptosis related to P150-GFP. Rather, caspase activation was present in more of the untransfected cells than in those that were successfully transfected with P150-GFP. A similar result was seen when HEK293 cells were transfected with P150-GFP. While there was a higher number of cells with activated caspases in the culture of P150-GFP transfected cells versus mock transfected cells, very few of the caspase-active cells (roughly 10%) overlap with successfully transfected cells producing GFP. While these results indicate that P150-GFP did not activate caspases in the cell, we could not explain the higher number of cells with activated caspases in the P150-GFP-transfected culture.

The lack of induction of apoptosis by P150 apparent in the caspase activation experiments was confirmed by the lack of chromatin fragmentation in these cell lines transfected with P150-GFP. A549 cells that had been transfected with GFP exhibited the same level of fragmentation as, if not more than, those transfected with P150-GFP indicating that P150 is no more toxic to these cells than either the transfection reagent itself or GFP. Likewise, P150 did not induce chromatin fragmentation in HEK293 cells any more than GFP did, once again demonstrating a lack of elevated cytotoxicity that could be attributed to P150 alone. The spurious induction of apoptosis in cells neighboring the P150-GFP transfected cells observed in the caspase activation assay was not observed using the TUNEL assay. Because P150 gave no indications of inducing apoptosis in human cells, it was unnecessary to investigate whether C would be able to neutralize induction of apoptosis.

FACS analysis showed that both HEK293 and A549 cells that have been transfected with either GFP or P150-GFP showed no indication of cell cycle arrest, similar to Vero cells transfected with these plasmids. Instead, P150- or GFP-transfected HEK293 cells exhibited normal cell cycle progression with no suggestion of arrest in G_2 or an inability to divide. Likewise, A549 cells, whether mock transfected or transfected with GFP or P150, also exhibited normal cell cycle progression. However, since these cells were near confluency at the time of transfection with P150-GFP, as were the Vero cells, we do not know if inhibition of the cell cycle would be observed if the cells were actively dividing at the time of transfection.

The lack of apoptosis induced in human cells could be attributed to a number of factors, one being the presence of a functional interferon system in these cells that Vero cells lack. However, studies by other laboratories have shown that apoptosis in response to RUBV infection varies among cell lines and that BHK cells, which also lack a functional interferon system, do

not exhibit RUBV induced CPE due to apoptosis [77]. A recent study investigating apoptosis induction by infection with RUBV in fetal and adult human cells used microchip analysis to investigate which genes were regulated by RUBV, and both pro- and anti-apoptotic genes were affected in cells infected with this virus. In this and a previous study, the adult cells were found to undergo apoptosis while the fetal cells did not. Both fetal and adult cells exhibited a robust interferon response, lending support to the idea that simply having an active interferon system within the host cell does not make a large difference in whether apoptotic pathways are triggered or not [66].

The question that remains then is how exactly the RUBV P150 protein is able to induce apoptosis in Vero cells to such an extraordinary level. It has been established through experimentation with UV-inactivated RUBV that active replication is required for RUBV to induce apoptosis [76, 80] as well as normal cell growth and proliferation [75] lending weight to the hypothesis that RUBV induces apoptosis through the intrinsic pathways. The exact members of the pathways have not yet been definitively identified, however. While there has been some evidence of a p53-dependent pathway being activated [81] there is also evidence countering this and supporting the theory that the Akt survival pathway and Bcl-2 pathways are more pivotal towards RUBV' activation of apoptosis in host cells [75, 77]. Without knowing the exact pathway activated, it is difficult to determine the exact mechanism employed by P150 for apoptosis induction, however towards answering this question multiple theories could be explored. The first theory that could be proposed is one of substrate confusion given that both caspases and P150 are cysteine proteases with His and Cys as members of their catalytic site [25, 67]. The action of effector caspases 3, 6, and 7 is reliant on their proteolytic cleavage and subsequent activation by initiator caspases 8, 9, and 10. Activation of these initiator caspases is

reliant upon proteolytic self-cleavage signaled by pro-apoptotic regulatory proteins. Previous studies with HIV-1 in Jurkat cells have demonstrated through SDS-PAGE the ability of HIV's protease (PR) to cleave procaspase-8. This cleavage also did not produce the exact same subunits as normal cleavage of procaspase-8 would. However, immunofluorescent labeling also showed that once cleaved through this mechanism the caspase was able to begin its signal cascade and amplification resulting in the induction apoptosis in these cells [68]. One primary difference between the HIV protease versus caspase and P150 is that while P150 and caspases are both cysteine proteases, PR is an aspartyl protease. The relevance of this is that even though P150 cleaves between two glycines while caspases cleave after an aspartic acid it could still be possible that P150 is able to cleave procaspase-8 in a manner similar to PR thus producing an active initiator caspase whose signal is amplified and induces apoptosis.

In conclusion, the results presented in this M.S. Thesis demonstrate that while P150 is capable of inducing apoptosis in Vero cells and that C is able to neutralize these apoptotic effects, these results are cell-type specific. Thus, if induction of apoptosis by RUBV contributes to CRS, it is in a cell-specific manner. RUBV replicons were able to induce a uniform cell cycle arrest in Vero cells typical of RUBV infection and this system is a candidate for studying the mechanisms behind this arrest, which are apparently not related to induction of apoptosis. However, given that aneuploidy has been linked to certain types of cancer [64] and thus there are cellular checkpoints to monitor and eliminate cells with aneuploidy, this theory should not be completely discarded. It stands to reason that this aneuploidy is triggering apoptosis and this could be the mechanism through which RUBV induces apoptosis leading to the developmental abnormalities witnessed in CRS. This theory has been substantiated by experimentation using knockout mice defective in a pivotal cell division signaling protein. These mice lack consistent

appropriate cell division and thus suffer apoptosis and developmental abnormalities [65]. Since G_2 arrest is also a hallmark of cancer as well as polyploidy [64] it could also be possible that it is the combined effects of polyploidy and arrest in G_2 that are sounding the anti-cancer alerts in the cell and instigating apoptosis. As with the induction of apoptosis, study of interference with the cell cycle needs to be extended to other cell types to see if it is cell type specific or a general phenomenon. Most importantly these studies need to be carried out in fetal cell lines. Thus far, RUBV has not been found to induce apoptosis in human fetal fibroblasts [81,66] and we found that P150 did not induce apoptosis in HEK 293, a fetal cell line. The variability in apoptosis induction depending on cell type could be a prime candidate to explain the specific types of damage encountered following fetal infection. It could also lend explanation as to why some aspects of CRS appear to be caused by apoptosis while others seem more necrotic in nature. Despite the inability of this study to truly identify specific molecular causes of CRS, it has shed light on a number of future directions that could be taken towards solving this enigmatic puzzle.

REFERENCES

1. Wesselhoeft, *Rubella and congenital deformities.* N. Engl. J. Med, 1949. **240**(7): p. 258-61.

2. Smith, J., *Contributions to the study of Rötheln.* 1881. **4**: p. 14.

3. Lee, J.Y. and D.S. Bowden, *RUBV replication and links to teratogenicity.* Clin Microbiol Rev, 2000. **13**(4): p. 571-87.

4. Plotkin SA, W.O., *Vaccines. 3rd Edition. Philadelphia: W.B. Saunders Compant, 1998. 222-293, 409-441 and 508-531. and B.N. Fields, ed. Fields Virology 3rd edition. Philadelphia: Lippincott-Raven Publishers, 1996. 1:1177-1313, 899-931.*

5. Atkinson W, H.J., McIntyre L, Wolfe S, *"Chapter 12. Rubella", Epidemiology and Prevention of Vaccine-Preventable Diseases. 10th ed.* 2007: Centers for Disease Control and Prevention.

6. Ackerknecht, E.H., *A short history of medicine.* Johns Hopkins University Press, 1982. **129**.

7. . Best, J.M., Cooray, S., Banatvala J.E. , *Rubella* Topley and Wilson's Microbiology and Microbial Infections, 2005. **2**: p. 960-992.

8. Hess, A.F., *German measles (rubella): an experimental study.* The Archives of Internal Medicine 1914. **13**: p. 913-916.

9. Best, J.B., JE. Rubella. In: Zuckerman, A. J., Banatvala, J. E. and Pattison JR. , editor. Principles and practice of clinical virology. 4th. Chichester, John Wiley & Sons Ltd; 2000. pp. 387–418.

10. Gregg, N., *Congenital cataract following German Measles in the mother.* Opthalmol Society, 1941. **3**: p. 35-46.

11. Parkman, P.D., E.L. Buescher, and M.S. Artenstein, *Recovery of RUBV from army recruits.* Proc Soc Exp Biol Med, 1962. **111**: p. 225-30.

12. Weller, T.H. and F.A. Neva, *Biological Characteristics of RUBV as Assayed in a Human Amnion Culture System.* Arch Gesamte Virusforsch, 1965. **16**: p. 393-400.

13. Frey, T.K., *Molecular biology of RUBV.* Adv Virus Res, 1994. **44**: p. 69-160.

14. Hemphill, M.L., et al., *Time course of virus-specific macromolecular synthesis during RUBV infection in Vero cells.* Virology, 1988. **162**(1): p. 65-75.

15. Atreya, C.D., K.V. Mohan, and S. Kulkarni, *RUBV and birth defects: molecular insights into the viral teratogenesis at the cellular level.* Birth Defects Res A Clin Mol Teratol, 2004. **70**(7): p. 431-7.

16. Webster, W., *Teratogen Update: Congenital Rubella.* Teratology, 1998. **58**: p. 13-23.

17. Coyle, P.K.W., J Buimovici-Klein, E Moucha, R Cooper, L, *Rubella-Specific Immune Complexes After Congenital Infection and Vaccination.* Infection and Immunity, 1982. **36**(2): p. 498-503.

18. Miller, E.C.-W., J.E., Pollock, T.M., *Consequences of confirmed maternal rubella at successive stages of pregnancy.* Lancet, 1982. **2**(781-784).

19. Williams, M.P.B., T. A. Riggs, H. G Roehrig, J. T., *Characteristics of a Persistent Rubella Infection in a Human Cell Line.* J. gen Virol, 1981. **52**: p. 321-328.

20. Abernathy, E.S., C.Y. Wang, and T.K. Frey, *Effect of antiviral antibody on maintenance of long-term RUBV persistent infection in Vero cells.* J Virol, 1990. **64**(10): p. 5183-7.

21. Pugachev, K.V. and T.K. Frey, *RUBV induces apoptosis in culture cells.* Virology, 1998. **250**(2): p. 359-70.

22. Yoneda, T.U., M Sakuda, M Miyazaki, T, *Altered growth, differentiation, and responsiveness to epidermal growth factor of human embryonic mesenchymal cells of palate by persistent RUBV infection.* J. Clin. Invest, 1986. **77**: p. 1613-1621.

23. Plotkin
, S.A. and A. Vaheri, *Human fibroblasts infected with RUBV produce a growth inhibitor.* Science, 1967. **156**(3775): p. 659-61.

24. Baron, M.F., K, *Oligomerization of the structural proteins of RUBV.* Virology, 1991. **185**: p. 811-819.

25. Liu, Z.Y., D Qui, Z Lim, KT Chong, P Gillam, S, *Identification of domains in RUBV genomic RNA and capsid protein necessary for specific interaction.* Journal of Virology, 1996. **70**: p. 2184-2190.

26. Tzeng, W.P. and T.K. Frey, *RUBV capsid protein modulation of viral genomic and subgenomic RNA synthesis.* Virology, 2005. **337**(2): p. 327-34.

27. Beatch, M.D.a.H.T.C., *RUBV capsid associates with host cell protein p32 and localizes to mitochondria.* Journal of Virology, 2000. **74**(12): p. 5569-76.

28. Law, L.J., et al., *Analyses of phosphorylation events in the RUBV capsid protein: role in early replication events.* J Virol, 2006. **80**(14): p. 6917-25.

29. Kujala, P.A., T Ehsani, N Auvinen, P Vihinen, H Kaariainen, L, *Intacellular distribution of RUBV nonstructural protein P150.* Journal of Virology, 1999. **73**(9): p. 7805-11.

30. Wang, X. and S. Gillam, *Mutations in the GDD motif of RUBV putative RNA-dependent RNA polymerase affect virus replication.* Virology, 2001. **285**(2): p. 322-31.

31. Atreya, C.D.K., S. Mohan K, *RUBV P90 associates with the cytokinesis regulatory protein Citron-K kinase and the viral infection and constitutive expression of P90 protein both induce cell cycle arrest following S phase in cell culture.* Archives of Virology, 2004. **149**: p. 779-789.

32. Chen, J.S., JH Strauss, EG Frey, TK, *Characterization of the RUBV nonstructural protease domain and its cleavage site.* J Virol, 1996. **70**: p. 4707-13.

33. Liu, X.R., SL Jackson, RJ Frey TK, *The RUBV nonstructural protease requires divalent cations for activity and functions in trans.* J Virol, 1998. **72**: p. 4463-66.

34. Tzeng, W.P. and T.K. Frey, *Complementation of a deletion in the RUBV p150 nonstructural protein by the viral capsid protein.* J Virol, 2003. **77**(17): p. 9502-10.

35. Pugachev, K.V., E.S. Abernathy, and T.K. Frey, *Improvement of the specific infectivity of the RUBV (RUB) infectious clone: determinants of cytopathogenicity induced by RUB map to the nonstructural proteins.* J Virol, 1997. **71**(1): p. 562-8.

36. Mifune, K.D., J Rawls, WE, Infection and Immunity, 1970. **2**: p. 132-138.

37. Vaheri, A.S., WD Plotkin, SA Maes, R, Virology, 1965. **27**: p. 239-241.

38. Petruzziello, R., et al., *Pathway of RUBV infectious entry into Vero cells.* J Gen Virol, 1996. **77 (Pt 2)**: p. 303-8.

39. Katow, S.S., A, J Gen Virol, 1988. **69**: p. 2797-2807.

40. Lee, J.Y., *Morphological and functional analysis of RUBV*. 1993, University of Melbourne: Melbourne, Australia.

41. Pugachev, K.V. and T.K. Frey, *Effects of defined mutations in the 5' nontranslated region of RUBV genomic RNA on virus viability and macromolecule synthesis.* J Virol, 1998. **72**(1): p. 641-50.

42. Oker-Blom, C., *The gene order of RUBV structural proteins is NH_2-C-E2-E1-COOH.* J Virol, 1984. **51**: p. 354-358.

43. Frey, T.K.M., LD, *Sequence of the region coding for virion proteins C and E2 and the carboxy terminus of the nonstructural proteins of RUBV: comparison with alphaviruses.* Gene, 1988. **62**: p. 85-99.

44. Hobman, T.C.S., R Gillam, S, *Translocation of RUBV glycoprotein E1 into the endoplasmic reticulum.* J Virol, 1988. **62**: p. 4259-64.

45. Waxham, M.W., J, *Detailed immunologic analysis of the structural polypeptides of RUBV using monoclonal antibodies.* Virology, 1985. **143**: p. 153-165.

46. Wolinsky, J., *Rubella, p. 899-929. In Fields, BN Knipe, DM Howley, PM Chanock, RM Melnick, JL Roizman, B (ed.), Virology, 3rd ed., vol. 1. Lipincott-Raven Publishers, Philadelphia, Pa.* 1996.

47. Holmes, I.W., MC Jack, I Grutner, J, *Identification of two possible virus particles in rubella-infected cell.* J Gen Virol, 1968. **2**: p. 37-42.

48. Holmes, I.W., MC Warburton, MF *Is rubella an arbovirus. II. Ultrastructural morphology and developement.* Virology, 1969. **37**: p. 15-25.

49. Lee, J.Y.M., JA Bowden, DS, *Replication complexes associated with morphogenesis of RUBV.* Archives of Virology, 1992. **122**: p. 95-106.

50. Lee, J.Y.M., JA Bowden, DS, *Characterization of RUBV replication complexes using antibodies to double-stranded RNA.* Virology, 1994. **200**: p. 307-312.

51. Lee, J.Y.M., JA Bowden, DS, *Localization of RUBV core particles in Vero cells.* Virology, 1999. **265**: p. 110-119.

52. Bree RT, S.-C.C., Grealy M, Byrnes L, Gorman AM, Samali A, *Cellular longevity: role of apoptosis and replicative senescence.* Biogerontology, 2002. **3**: p. 195-206.

53. Ziegler U, G.P., *Morphological features of cell death.* News Physiol Sci, 2004. **19**: p. 124-128.

54. Fulda S, D.K., *Extrinsic versus intrinsic apoptosis pathways in anticancer chemotherapy.* Oncogene, 2006. **25**: p. 4798-4811.

55. Ghobrial IM, W.T., Adjei AA, *Targeting apoptosis pathways in cancer.* CA Cancer J Clin, 2005. **55**: p. 178-194.

56. Thornberry NA, L.Y., *Caspases: enemies within.* Science, 1998. **281**: p. 1312-1316.

57. Lavrik IN, G.A., Krammer PH, *Caspases: pharmacological manipulation of cell death.* J Clin Invest, 2005. **115**: p. 2665-2672.

58. Haanen C, V.I., *Apoptosis: Programmed cell death in fetal development.* Obstetrics & Gynecology, 1996. **64**: p. 129-133.

59. Cho A, C.D., Langille BL, *Apoptosis (Programmed Cell Death) in arteries of the neonatal lamb.* Circ Res, 1995. **76**: p. 168-175.

60. Lee KKH, C.W., *Hitogenic potential of rat hind-limb inter-digital tissues prior to and during the onset of prtammed cell death.* Anat Rec, 1993. **236**(568-572).

61. Terada T, N.Y., *Detection of apoptosis and expression of apoptosis-related proteins during human intrahepatic bile duct development.* American Journal of Pathology, 1995. **146**: p. 67-74.

62. Brill A, T.A., Carp H, Toder V, *The Role of Apoptosis in Normal and Abnormal Embryonic Development.* Journal of Assisted Reproduction and Genetics, 1999. **16**(10): p. 512-519.

63. Fontana, J., et al., *Novel replication complex architecture in rubella replicon-transfected cells.* Cell Microbiol, 2007. **9**(4): p. 875-90.

64. Nunez R, G.N., Villafane C, Bruno A, Lindgren V, *Description of a flow cytometry approach based on SYBR-14 staining for the assessment of DNA content, cell cycle analysis, and sortin of living and neoplastic cells.* Experimental and Molecular Pathology, 2004. **76**: p. 29-36.

65. Di Cunto F, I.S., Hirsch E, Broccoli V, Bulfone A, Migheli A, Atszori C, Turco E, Triolo R, Dotto GP, Silengo L, Altruda F, *Defective neurogenesis in citron kinase knockout mice by altering cytokinesis and massive apoptosis.* Neuron, 2000. **28**: p. 115-127.

66. Adamo P, Z.M., Frey TK, *Analysis of gene expression in fetal and adult cells infected with RUBV.* Virology, 2007. **370**: p. 1-11.

67. Nicholson, D., *Caspase structure, proteolytic substrates, and function during apoptotic cell death.* Cell Death and Differentiation, 1999. **6**: p. 1028-1042.

68. Nie Z, B.G., Vlahakis S, Schimnich A, Brenchley J, Trushin S, Warren S, Schnepple D, Kovacs C, Loutfy M, Douek D, Badley A, *Human Immunodeficiency Virus Type 1 Protease Cleaves Procaspase 8 IN Vivo.* Journal of Virology, 2007. **81**(13): p. 6947-6956.

69. Goffe, A. *A diploid human cell strain with chronic inapparent rubella infection.* Archiv fur die Gesamte Virusforschung, 1965. **16**: p. 469.

70. Joklik, W. K. (1977). *Mechanisms of establishment and maintenance of persistent infections*. Microbiology-1977 434-438. Edited by D. Schlessinger. Washington D. C.: American Society for Microbiology.

71. Maasab HF, Veronelli JA. *Characteristics of serially propagated monkey kidney cell cultures with persistent rubella infection.* Journal of Bacteriology, 1966. **91**: p. 436-441.

72. Norval M. *Mechanism of persistence of RUBV in LLC-MK$_2$ cells.* Journal of General Virology, 1979. **43**: p. 289-298.

73. Sato M, Tanaka H, Yamada T, Yamamoto N. *Persistent infection of BHK-21/WI-2 cells with RUBV and characterization of rubella variants*. Archives of Virology, 1977. **54**: p.333-343.

74. Svedmyr A. *Persistent infection with RUBV in RK-13 cells*. Archiv fur die Gesamte Virusforschung, 1965. **16**: p. 464-465.

75. Cooray S, Jin L, Best J. *The involvement of survival signaling pathways in RUBV induced apoptosis.* Virology Journal, 2005. **2.**

76. Cooray S, Best J, Jin L. *Time-course induction of apoptosis by wild-type and attenuated strains of RUBV.* Journal of General Virology, 2003. **84:** p. 1275-1279.

77. Duncan R, Muller J, Lee N, Esmaili A, Nakhasi H. *RUBV-induced apoptosis varies among cell lines and is modulated by Bcl-X and caspase inhibitors.* Virology, 1999. **255**: p. 117-128.

78. Duncan R, Esmaili A, Law L, Bertholet S, Hough S, Hobman T, Nakhasi H. *RUBV capsid protein induces apoptosis in transfected RK13 cells.* Virology, 2000. **275**, p. 20-29.

79. Domegan L, Atkins G. *Apoptosis induction by the Therien and vaccine RA27/3 strains of RUBV causes depletion of oligodendrocytes from rat neural cell cultures.* Journal of General Virology, 2002. **83**: p. 2135-2143.

80. Hofmann J, Pletz M, Liebert U. *RUBV-induced cytopathic effect in vitro is caused by apoptosis.* Journal of General Virology, 1999. **80**: p. 1657-1664.

81. Megyeri K, Berencsi K, Halazonetis T, Prendergast G, Gri G, Plotkin S, Rovera G, Gonczol E. *Involvement of a P53-dependent pathway in RUBV-induced apoptosis.* Virology, 1999. **259**: p.74-94.

82. Petrakova O, Volkova E, Gorchakov R, Paessler S, Kinney R, Frolov I. *Noncytopathic replication of Venezuelan Equine Encephalitis Virus and Eastern Equine Encephalitis Virus Replicons in Mammalian Cells.* Journal of Virology, 2005. **79**: p. 7597-7608.

83. Nakhasi HL, Zheng D, Hewlett K, Liu T. *RUBV replication: effect on interferon and actinomycin D.* Virus Res, 1988. **10**: p. 1-15.

84. Nakhasi HL, Rouault A, Jaile D, Liu T, Klausner R. *Specific high affinity binding of host cell proteins to the 3' regions of RUBV RNA.* New Bio, 1990. **2**: p. 255-264.

85. Nakhasi HL, Cao X, Rouault A, Liu T. *Specific bind of host cell proteins to the 3' terminal stem loop structure of RUBV negative-strand RNA.* Journal of Virology, 1991. **65**: p. 5961-5967.